# ASSESSMENT OF THE HYDRAULIC PERFORMANCE OF THE WNP-1 CONTAINMENT RECIRCULATION SUMPS

## HYDRAULIC EVALUATION OF THE DESIGN OF CONTAINMENT RECIRCULATION SUMPS


by

Mahadevan Padmanabhan


## HYDRAULIC MODEL STUDY OF CONTAINMENT RECIRCULATION SUMPS


by

William W. Durgin
John F. Noreika


WASHINGTON PUBLIC POWER SUPPLY SYSTEM
NUCLEAR PROJECT NU.BER 1
(WNP-1)

Prepared for

United Engineers & Constructors, Inc.


GEORGE E. HECKER, DIRECTOR

ALDEN RESEARCH LABORATORY

WORCESTER POLYTECHNIC INSTITUTE

HOLDEN, MASSACHUSETTS


December 1982

## EXECUTIVE SUMMARY

Alden Research Laboratory was contracted by United Engineers & Constructors, Inc. (UE&C) to evaluate the hydraulic performance of the Containment Recirculation Sumps of the Washington Public Power Supply System Nuclear Project No.1 (WNP-1). Two investigations were conducted, the first, "Hydraulic Evaluation of the Design of Containment Recirculation Sumps," was performed utilizing existing literature, results from previous model studies, and results from on-going research projects. The second evaluation, "Hydraulic Model Study of Containment Recirculation Sumps," was performed by constructing and testing a 1:2.5 scale model of DHR and CSS containment sumps. Each evaluation analyzed the potential adverse flow conditions which could result from vortex activity, excessive swirling flow, and large inlet losses.

The results from the initial investigation indicated that the screens and gratings would probably be sufficient to prevent formation of air-drawing vortices under normal operating conditions and under extreme screen blockage situations. This prediction was confirmed by the model study results. Air drawing vortices did not occur under any test conditions; the maximum vortices encountered were classified as surface dimples. From the available literature, it was concluded that swirl angles up to ten degrees could develop in the suction pipe inlets. The model results indicated a maximum swirl angle of 13.5 degrees and an average angle of 9.96 degrees in the CSS sump and a maximum swirl angle of 6.61 degrees and average swirl angle of 2.60 degrees for the DHR sump. These swirl angles are not considered excessive, especially since pipe friction losses will greatly reduce these values before the flow reaches the recirculation pumps. The overall inlet loss coefficients were predicted to have values of approximately 0.35. The measured values were lower in the model study. Average loss coefficients for the DHR and CSS sump were measured as 0.06 and 0.15, respectively.

The results of the model study in conjunction with the hydraulic evaluation and the literature pertaining to scale effects indicate that the prototype will not experience air entrainment due to free surface vortices.

Furthermore, the loss coefficients reported herein can be used in conjunction with pump performance data to evaluate the sufficiency of available net positive suction head (NPSH). Considering the decay of swirl in the outlet lines, even the highest measured values would be reduced to less than 2 degrees over the pipe length. Typically, degradation of pump performance for such small swirl angles is insignificant.

In-plant pre-operational testing of the containment sumps would be unlikely to add significantly to the findings presented herein. In fact, due to the difficulty of conducting such tests and associated measurements, it is likely that they would be less conclusive.

Both reports, "Hydraulic Evaluation of the Design of Containment Recirculation Sumps," and "Hydraulic Model Study of Containment Recirculation Sumps," are bound in this single volume.

# HYDRAULIC EVALUATION OF THE DESIGN OF CONTAINMENT RECIRCULATION SUMPS

## WASHINGTON PUBLIC POWER SUPPLY SYSTEM NUCLEAR PROJECT 1 (WNP-1)

by

Mahadevan Padmanabhan

Report Submitted to

United Engineers and Constructors, Inc.

George E. Hecker, Director

ALDEN RESEARCH LABORATORY

WORCESTER POLYTECHNIC INSTITUTE

HOLDEN, MASSACHUSETTS

June 1982

ABSTRACT

A hydraulic evaluation of the design of the containment recirculation sumps of the Washington Public Power Supply System (WPPSS) Nuclear Project 1 (WNP-1) has been performed, based on available literature on related topics, results of hydraulic model studies of similar sumps conducted at the Alden Research Laboratory (ARL) of Worcester Polytechnic Institute (WPI) or elsewhere, and the experience and available results from the ongoing full scale containment sump studies at ARL (25).

The evaluation indicated no air-entraining vortices would likely occur for the WNP-1 sumps with nearly uniform approach flows for the operating ranges of flows and water levels. With extreme flow perturbations due to possible screen blockages of up to 75%, air-entraining vortices may form outside the sump screens, but are likely to be suppressed by the screens and gratings, the sump solid top cover being submerged even under minimum water levels. However, the extent to which vortices may be suppressed cannot be predicted with certainty and a limited hydraulic model study to investigate this aspect may be appropriate. In any case, no significant air-entraining vortices drawing more than 2% air (void fractions) may be expected, even under possible approach flow perturbations. Since the sump location is outside the shield wall and far away from any likely LOCA locations, no possibility of air ingestion or other problems due to jet impact is indicated.

Flow rotation of about 10 degree swirl angle near the pipe inlet may be possible, but this swirl would decay considerably, to less than about 2 degrees at the pump location, due to pipe friction over the long straight pipe lengths available upstream from the pumps.

The overall inlet losses are estimated to be small. Including the racks, screen, and pipe entrance losses, the overall inlet loss coefficient is expected to have a value of about 0.35, and hence, should not have any significant impact on the available Net Positive Suction Head (NPSH) for the recirculation pumps. For the WNP-1 system, the available NPSH is reported to be higher than the required NPSH by about 8 ft.

# TABLE OF CONTENTS

## 1.0 INTRODUCTION

In the event of a loss of coolant accident (LOCA) in a nuclear power station, the emergency core cooling system (ECCS), involving decay heat removal (DHR) and containment spray systems (CSS), would be activated to supply coolant to the reactor core and vessel to dissipate the residual heat and to the CSS to reduce containment pressure. At first, the pumps of these systems draw water from a large Borated Water Storage Tank (BWST). When the water level in BWST reaches a pre-determined level, the pumps are switched to a recirculating mode, drawing water that has accumulated on the containment floor through a containment recirculation sump. The systems are expected to operate for extended periods of time in this mode. Containment recirculation sumps are provided in the containment floor to collect water and supply it to the ECCS pumps, to screen out debris, and to provide sufficient suction head for the pumps. Hence, they form a key flow link in providing emergency coolant to the reactor, and in providing control of the containment environment during the recirculation mode.

The flow patterns within the containment sump influence the character of the flow in lines leading to the safety system pumps. Of primary concern is the tendency for air-entraining vortices to form, either because of the approach flow pattern and sump geometry, or because of local swirl initiation by, for example, asymmetrical debris blockage of the racks and screens. Additionally, direct impingement of jets in the sump area, as might be caused by a nearby main coolant pipe break, might also contribute to poor sump performance, especially for shallow sumps. Specifically, the major items of concern regarding the containment sump performance are:

1. Entrained Air - Air entrainment in the suction lines could be due to air entraining vortices existing in the sump, or due to air entrainment generated by water or steam jets from the break impinging near the sump through the free water surface. It has been found that air concentrations of greater than about 3 percent by volume in a suction line can lower the head-discharge curves of centrifugal pumps considerably, causing lower pump capacities at a given head [1, 2, 3].

2. Swirl - Approach flow patterns, together with possible asymmetrical screen blockage, could induce a swirling flow in the sump area. This swirl could be transmitted to the suction pipe and might increase the losses at the intake [4]. Swirling flow in suction pipes could also affect the performance of pumps located close to the sump, depending on the intensity of swirl.

3. Losses Leading to Insufficient Net Positive Suction Head (NPSH) - A poorly designed sump could result in excessive head losses. Entrance losses caused by swirling flow, pipe inlet geometry, and vortex suppressors, may add up to a value such that the required NPSH of the pump is not satisfied, especially if available submergence is relatively low. It may be noted that the water temperature also affects the NPSH due to changes in vapor pressure. If a high submergence is available, the effects of inlet losses on available NPSH are less significant.

The Alden Research Laboratory (ARL) of Worcester Polytechnic Institute (WPI) was contracted by United Engineers & Constructors, Inc. (UE&C) to perform a hydraulic evaluation of the design of the containment recirculation sumps of Washington Public Power Supply System, Project 1 (WNP-1). The purpose of the evaluation is to investigate the likely hydraulic performance of the sump in light of the concerns described in the previous paragraphs.

The evaluation has been performed based on the available literature on related topics, results of model studies on similar sumps conducted at ARL and elsewhere, and the information available from the ongoing full scale study at ARL on containment sump reliability for the Department of Energy (DOE) and the Nuclear Regulatory Commission (NRC). The probability for vortexing and the magnitude of pipe swirl, air-withdrawal, and inlet losses are evaluated and results presented in this report.

This report is a preliminary technical evaluation of the hydraulic performance of WNP-1 containment sumps, submitted to UE&C as an ingredient in deciding whether additional evaluation of the sump performance through a hydraulic model study is needed.

## 2.0 SYSTEM DESCRIPTION

The containment recirculation sumps are located in the containment annulus between the ring (shield) wall and the containment outer wall, encompassing an arc of 81.5 degrees, the sump centerline being at a 68 ft radius (Figure 1). Separated into two independent trains or sump areas by a concrete wall 6 ft high, each sump area contains two depressed pits, one accommodating the suction pipe outlet leading to pumps of the Containment Spray System (CSS), while the other sump contains the suction pipe outlet for the pumps of the Decay Heat Removal System (DHR). Each of the sumps is 7 ft wide, with a floor elevation of 405 ft, and encompasses an arc of 36.5 degrees.

The depressed sump floors are sloping, with the lowest point at elevation 399'-1". Each of the DHR depressed sumps are about 7 ft x 6.5 ft, while the CSS depressed sumps are about 7 ft x 5.5 ft, both approximately 5 ft deep. The DHR suction pipes are 20 inches in diameter, located at a centerline elevation of 401'-5", while CSS suction pipes are 16 inches in diameter, located at a centerline elevation of 401'-3", both pipes oriented horizontally.

The maximum flow through the CSS suction pipes and DHR suction pipes are 3000 gpm/pipe and 6000 gpm/pipe, respectively. The water level in the sump area varies from elevation 410.84 ft to elevation 415 ft, providing a minimum pipe submergence of about 9.5 ft. The water temperature in the pressurized containment building could vary from a maximum of 255°F to a minimum of 55°F.

Each sump is provided with an 8 inch x 4 inch (high) curb on which rests a fine mesh screen and a trashrack 4 ft 4 inches high. A sloping solid deck plate is over the entire sump area, with a low point at elevation 409'11-1/2" (Figure 2). The solid deck plate is submerged at the minimum water level of 410.84 ft.

Table 1 summarizes the data relative to the sump supplied by UE&C, and this information is used for the evaluation of the sump design, along with relevant drawings supplied by UE&C.

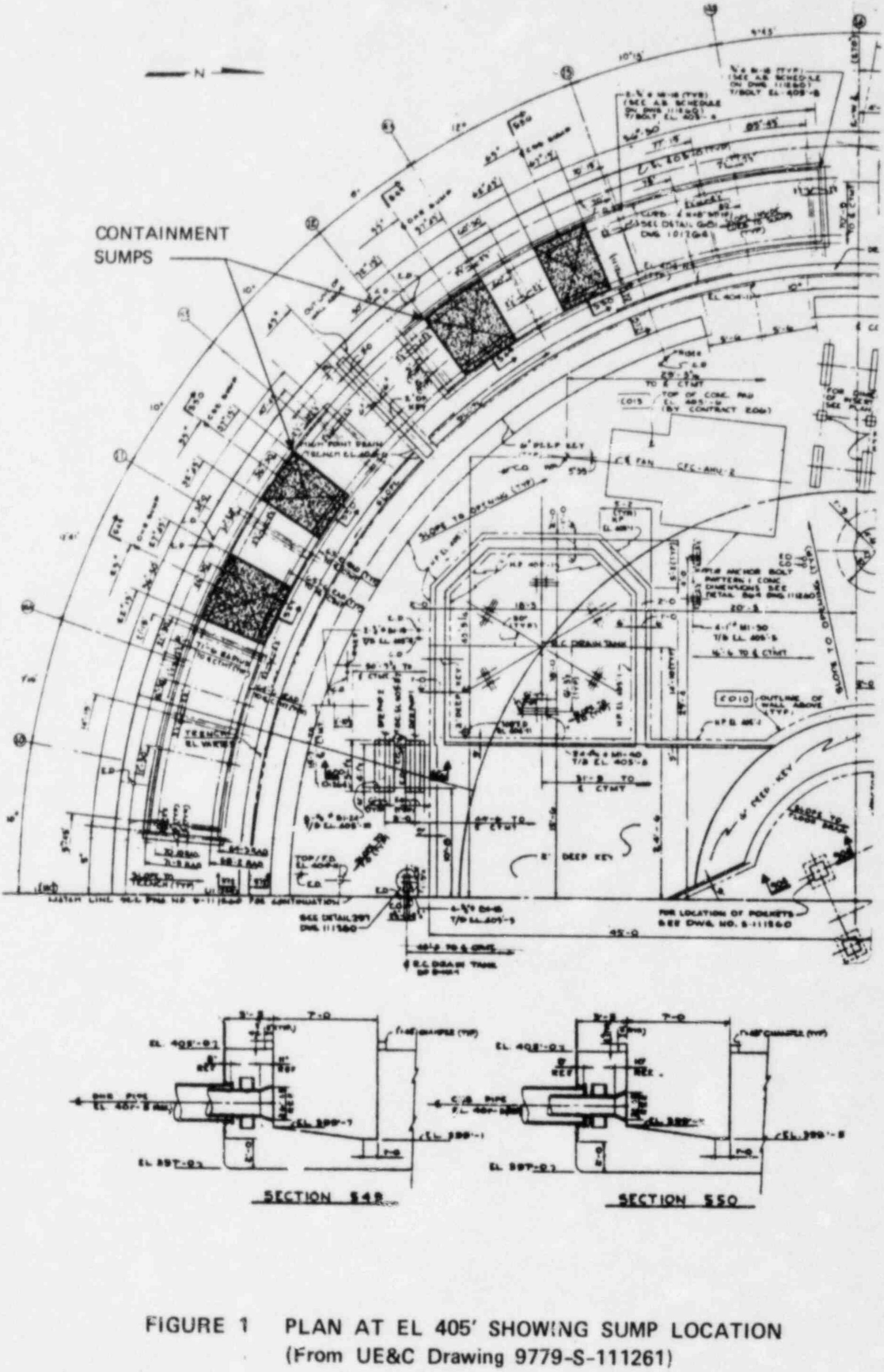


FIGURE 1 PLAN AT EL 405' SHOWING SUMP LOCATION
(From UE&C Drawing 9779-S-111261)

ARL

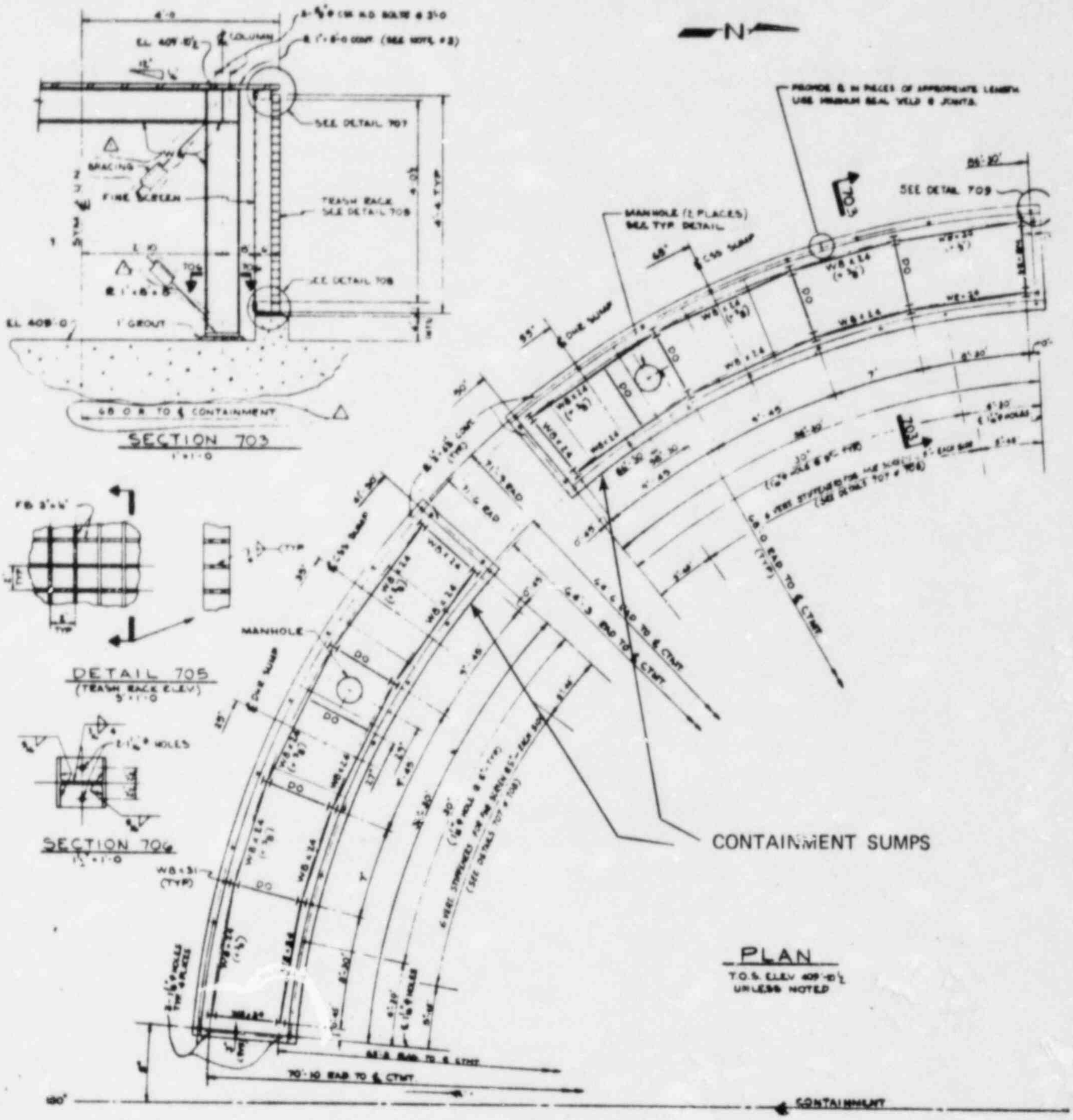


FIGURE 2 CONTAINMENT SUMP DETAILS
(From UE&C Drawing 9779-F-101378)

# TABLE 1

## WNP-1 Containment Sump Data

### Sump Water

Water Levels - Maximum EL 415.00'
Minimum EL 410.84'

Water Temperature - Maximum 255°F
Minimum 55°F

pH - 8.3 to 9.3

| Sumps | DHR | CSS |
|---|---|---|
| Number | 2 | 2 |
| Size (approx.) | 7' x 6'6" x 5' (depth) | 7' x 5'6" x 5' (depth) |
| Bottom EL | EL 399'-7" | EL 399'-11" |
| Suction Pipe Diameter | 20" | 16" |
| Centerline Elevation | EL 401'-5" | EL 401'-3" |

| Trashracks and Screens | Trashrack | Screen |
|---|---|---|
| Material | A-36 Steel | Stainless Steel Series 300 |
| Overall Size, Trashrack Bar Spacing | See Drawing No. 9779-F-101378 for details | |
| Mesh | Mesh per linear inch = 9-1/2<br>Diameter of wire = 0.032"<br>Width of opening = 0.0733" | |
| Solid Deck Plate | 1" thick stainless steel<br>EL of top of deck = EL 409'-11-1/2" | |

| Pumps | DHR | CSS |
|---|---|---|
| Number | 2 (1 per train) | 2 (1 per train) |
| Type | Horizontal Single Stage | Horizontal Single Stage |
| Location | Gen'l. Serv. Bldg. EL 385' | Gen'l. Serv. Bldg. EL 385' |
| Capacity | 5,125 gpm @ 385'<br>6,375 gpm @ 270' | 3,000 gpm @ 530'<br>7,400 gpm @ 370' |
| Maximum Possible Flow Under Recirculation Mode | 6,00[illegible] gpm | 3,000 gpm |
| Design Temperature | 350°F | 300°F |
| Operating Temperature | | |
| Maximum | 305°F | 255°F |
| Minimum | 55°F | 55°F |
| NPSH Required at Centerline of Impeller | 14' @ 5,125 gpm | 12' @ 3,000 gpm |
| NPSH Available at Centerline of Impeller | 23.5' @ 6,000 gpm<br>(per UE&C prior to this evaluation) | 20' @ 3,000 gpm |

# 3.0 EVALUATION OF HYDRAULIC PERFORMANCE

Evaluation of the hydraulic performance of the WNP-1 containment recirculation sump is to be based on four performance indicators; namely, (a) Free-Surface Vortex Type; (b) Pipe Swirl; (c) Air-Withdrawn to Suction Pipes (due to air entraining vortices or otherwise); and (d) Inlet Losses (including rack and screen). The evaluation of each of the above performance indicators is accomplished using one or more of the following sources:

i) Available literature on vortexing and swirl;

ii) Test results of containment sump of similar geometry; and

iii) Information from the ongoing containment sump reliability studies with a full scale facility at ARL (for DOE and NRC through Sandia National Laboratories).

Details of the sump geometry and of the flow and submergence conditions of the WNP-1 sumps are obtained from the drawings and other documents supplied by UE&C with their Inquiry No. H.O. 60392 dated December 16, 1981. In the paragraphs to follow, each of the performance indicators will be evaluated separately, and a summary of the hydraulic performance will be provided in the next chapter.

## 3.1 Free Surface Vortexing

### 3.1.1 Available Literature

Fluid motions involving vortex formation in pump intakes have been studied by several investigators [4, 5, 6, 7, 8]. Anwar et al [5] have shown from principles of dimensional analysis that vortexing will be a function of several dimensionless parameters given by,

$$\text{Vortexing} = f\left(\frac{\Gamma d}{2\pi Q}, \frac{s}{d}, \frac{u}{\sqrt{gs}}, \frac{Q}{\nu s}, \frac{\rho u^2 s}{\sigma}\right)$$

where

$\Gamma$ = circulation = $2 \pi u_\theta r$ where $u_\theta$ is the tangential velocity at radius r from vortex axis

d = pipe diameter

Q = discharge through the pipe

s = submergence

u = pipe flow velocity

g = acceleration due to gravity

$\nu$ = kinematic viscosity of water

$\sigma$ = surface tension (air to water)

In the above relationship, $\Gamma d/2\pi Q$ is a circulation number ($N_\Gamma$), while $u/\sqrt{gs}$ is a Froude number ($F_s$), $Q/\nu s$ is a radial Reynolds number ($R_R$), and $\rho u^2 s/\sigma$ is a Weber number ($W_s$). Definitions of these numbers could be different depending on the independent variables used for the grouping in the dimensional analysis.

For example, some investigators use a Froude number, $F_d = u/\sqrt{gd}$, a pipe Reynolds number ($R_e$) defined as $ud/\nu$, and a Weber number ($W_d$) defined as $\rho u^2 d/\sigma$ and so on [4, 7]. The circulation number is indicative of the angular momentum imparted by the approach flow; Froude number is indicative of gravity force while Reynolds and Weber numbers are indicative of viscous and surface tension forces, respectively. The influence of the radial Reynolds number and Weber number may be considered negligible for $R_R$ greater than $3 \times 10^4$ and $W_s$ greater than $10^4$ [5]. Daggett and Keulegan [4] show that viscous effects are negligible for $R_e$ greater than $3.2 \times 10^4$. Jain et al [7] show that for $W_d$ greater than 120, surface tension effects are negligible. The ranges of each of these numbers for WNP-1 sump are given in Table 2, and it is reasonable to say that viscous and surface tension effects could be neglected and, hence,

$$\text{Vortexing} = f(N_\Gamma, F_s, s/d)$$

The greatest difficulty in predicting a maximum vortex type for a containment sump would be the determination of the maximum value of $N_\Gamma$, the circulation number. The circulation is dependent on approach flow velocities and distribution and, in the case of containment sumps, both of these factors could have numerous variations depending on the approach flow to the sump and the extent and patterns of screen blockages.

TABLE 2

Summary of Geometric and Flow Variables
WNP-1 Sumps

| | Quantity | DHR | CSS |
|---|---|---|---|
| 1. | Pipe Diameter, d, inch | 20 | 16 |
| 2. | Maximum Flow, Q, gpm<br>cfs | 6000<br>13.4 | 3000<br>6.7 |
| 3. | Maximum Pipe Flow Velocity, u, fps | 6.63 | 5.28 |
| 4. | Submergence from pipe Centerline, S, ft | 9.5 to 13.5 | |
| 5. | Froude Number, $F_s = u/\sqrt{gs}$ | 0.32 to 0.38 | 0.25 to 0.30 |
| 6. | Pipe Reynolds Number, $R_e = ud/\nu$ at 70°F | $11 \times 10^5$ | $7 \times 10^5$ |
| 7. | Radial Reynolds Number, $R_R = Q/\nu s$, at 70°F | $1.0 \times 10^5$ to $1.4 \times 10^5$ | $5 \times 10^4$ to $7 \times 10^4$ |
| 8. | Weber Number, $W_s = \rho u^2 s/\sigma$ at 70°F | $1.5 \times 10^5$ to $2.3 \times 10^5$ | $1.0 \times 10^5$ to $1.5 \times 10^5$ |
| 9. | Submergence Ratio, s/d | 5.9 to 8.5 | 7.5 to 10.6 |

If $N_\Gamma$, $F_s$, and s/d are known, a reasonable prediction of whether or not an air core vortex will occur is possible using relationships such as those given by Anwar et al [5], Jain et al [7], and Daggett and Keulegan [4].

For the WNP-1 sump, the minimum water level is above the sump solid cover, and assuming no air is collected below the cover, the free-surface vortexing could take place only outside the sump screens and gratings. This is a significant factor since screens and gratings are known to act as good vortex suppressors [9]. In general, from various model studies, "submerged top cover" sumps are known to have no major vortexing problems [10, 11]. Since it is not possible to exactly determine the extent of vortex suppression of these screens and gratings, the effect of vortex suppression due to screens and gratings will not be included for conservatism.

There are many published papers on vortexing at intakes, and these references give a critical submergence (for a given pipe or entrance diameter and flow velocity in the pipe) above which air-entraining vortices will not occur [12, 13, 14, 15]. The validity of a critical submergence is, in general, reasonable for pump intakes with uniform approach flows; that is, the circulation generated by the approach flows is small. For the WNP-1 sumps, the critical submergence for the maximum flow conditions would be less than 4 ft as predicted by any of the publications [12, 13, 14, 15], whereas the available minimum submergence is 9.5 ft. Hence, under generally uniform approach flow conditions, no air-entraining vortices are likely. However, in a containment sump, the approach flow may be far from uniform due to uncertain LOCA locations that govern the flow distribution to the sump and more importantly, the possible screen blockages that drastically alter the flow patterns and generate considerable local circulation.

The most severe flow conditions favoring a strong vortexing in a sump are when the approach flow is obstructed by partially blocked sump screens in ways which increase the circulation within the sump area [10,11]. In general, a sump that does not generate any air-core vortices under any possible screen blockage conditions would be considered as performing well in terms of free-surface vortexing. For the WNP-1 sumps, the right train (sump centerlines at 55° and 65°) is more likely to be subjected to stronger circulation than the left train (Figure 1) since the large opening in the shield wall would allow a non-uniform approach flow to approach the right sumps. Assuming up to 75% blockage of screens, screen blockage schemes as shown in Figure 3A and 3B would generate a strong circulation and a possible vortex in the DHR sump area. The scheme of Figure 3A assumes a vortex outside sump screens and gratings as will be the case with the solid top cover submerged. The scheme 3B assumes a vortex inside sump screens, as will be the case if no credit is taken for the submerged top cover or when a free-surface is available below the top cover due to air caught underneath the top cover as the sump was filled up. Schemes 3A and 3B are just two of the possible extreme cases wherein a strong circulation could be generated at the sump. Consider an operating point with the highest approach velocity in the area of the DHR sump with a minimum sump water level. It is assumed, conservatively, that the tangential velocity, $u_\theta$, at a distance of one-half of approach flow width from a possible vortex center, is approximately equal to the average approach flow velocity at that location (Figures 3A and 3B). In other words, at a distance "r" from a postulated vortex center, a circulation $\Gamma = 2\pi\ u_\theta\ r$, is assumed, $u_\theta$ being the average approach velocity.

As shown in Figures 3A and 3B, the value of $N_\Gamma$ as defined by Anwar <u>et al</u> [5] for the cases considered will be about 0.14 to 0.5. With the value of $C = F_s/\sqrt{2}$ of about 0.27 ($F_s$ from Table 2), and with s/d of about 6, it can be seen from Figure 4 that the postulated flow condition is in the region of strong vortexing, implying air-core vortexing.

Jain <u>et al</u> [7] define circulation number using submergence $(N_\Gamma)_s$ and with this definition, $(N_\Gamma)_s$ for the case of Figures 3A and 3B will be about 5.1 to 16.9. They also define Froude number with pipe diameter, and using $F_d = u/\sqrt{gd}$, $F_d$ is about 0.9. Figure 5, drawn from Jain <u>et al</u> [7], is a plot of $N_\Gamma^{0.84}\ F_d$ against K s/d, where K is a function of viscosity parameter $N = g^{1/2}\ d^{3/2}/\nu$. Although this figure was derived using vertical outlet data, it is reasonably valid for horizontal outlets. K would be about 1 if N is greater than $5 \times 10^4$, which is the case for the present sump. Referring to Figure 5, it is seen that the operating range considered (with s/d = 5.9) is in the region of air-entraining vortexing.

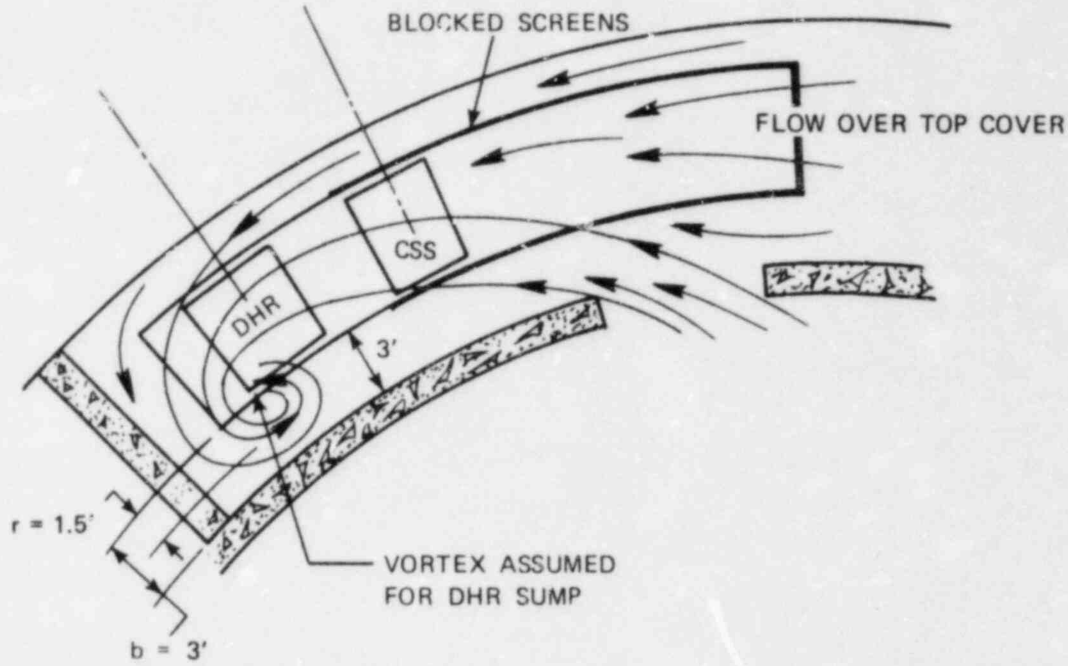


| | |
|---|---|
| Maximum Flow, Q, gpm | 6000 |
| Maximum Flow, Q, cfs | 13.4 |
| Approach Flow Depth, y, ft | 5.84 |
| $u_\theta$ = Q/b y, fps | 0.76 |
| r, distance at which $u_\theta$, the tangential velocity exists, ft | 1.5 |
| Circulation, $\Gamma = 2\pi\ u_\theta\ r$ | 7.21 |
| $N_\Gamma = \Gamma d/2\pi Q$ | 0.14 |
| $(N_\Gamma)_s = \Gamma s/Q$ | 5.11 |
| $(N_\Gamma)_A = \Gamma A/Q = \Gamma d/2Q$ | 0.43 |
| s/d | 5.9 |

**FIGURE 3A A SCREEN BLOCKAGE SCHEME LIKELY TO INDUCE STRONG CIRCULATION WITHIN SUMP AREA OUTSIDE SCREENS**

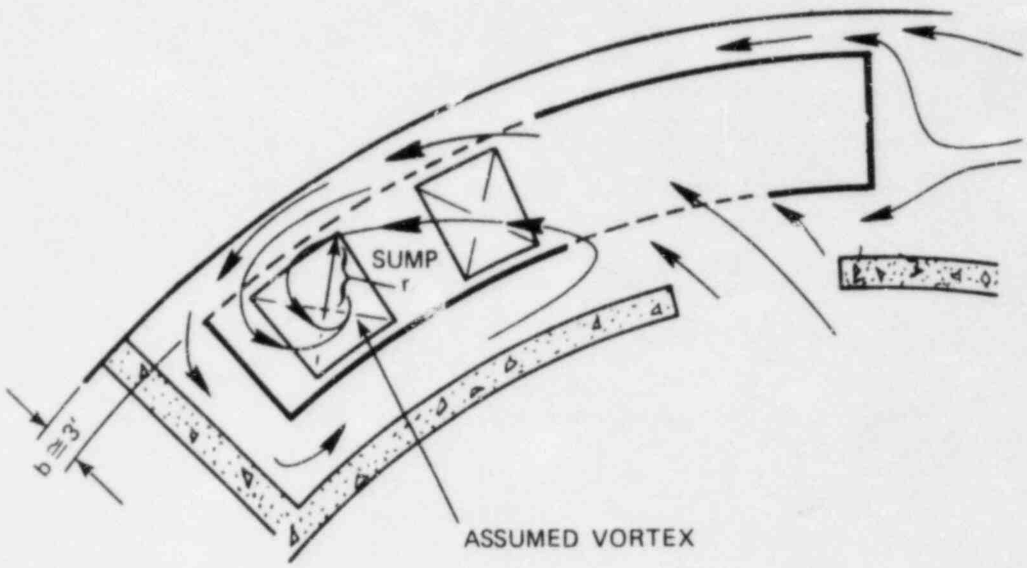


| | |
|---|---|
| Maximum Flow, Q, gpm | 6000 |
| Maximum Flow, Q, cfs | 13.4 |
| Approach Flow Depth, y, ft | 5.84 |
| $u_\theta$ = Q/b y, fps | 0.76 |
| r, distance at which $u_\theta$, the tangential velocity exists, ft | 5.0 |
| Circulation, $\Gamma = 2\pi\ u_\theta\ r$ | 23.9 |
| $N_\Gamma = \Gamma d/2\pi Q$ | 0.5 |
| $(N_\Gamma)_s = \Gamma s/Q$ | 16.9 |
| $(N_\Gamma)_A = \Gamma A/Q = \Gamma d/2Q$ | 1.5 |
| s/d | 5.9 |

FIGURE 3B A SCREEN BLOCKAGE SCHEME LIKELY TO INDUCE STRONG CIRCULATION WITHIN SUMP AREA INSIDE SCREENS

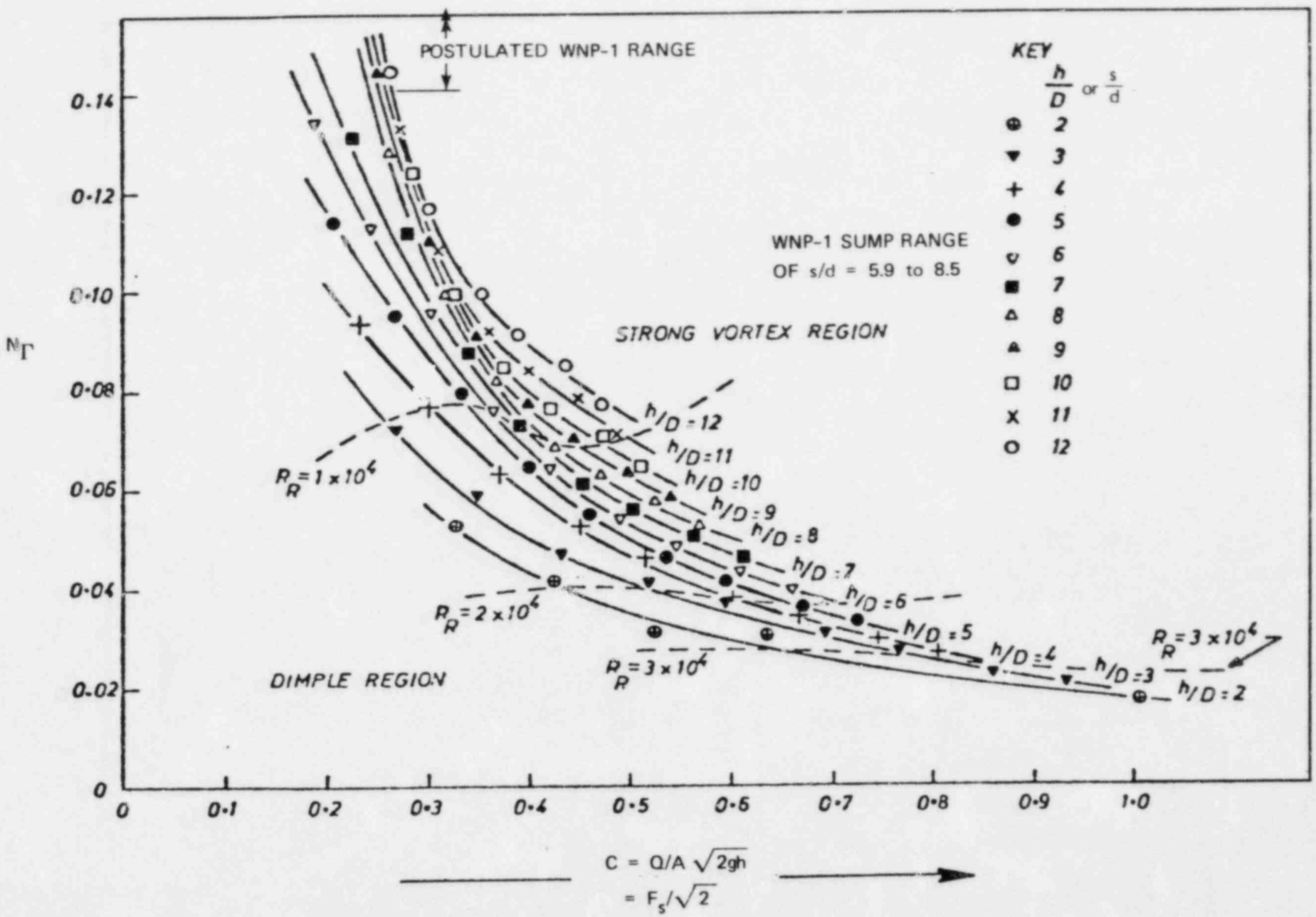


FIGURE 4 VORTEXING RANGE CURVE FROM ANWAR et al (5)

ARL

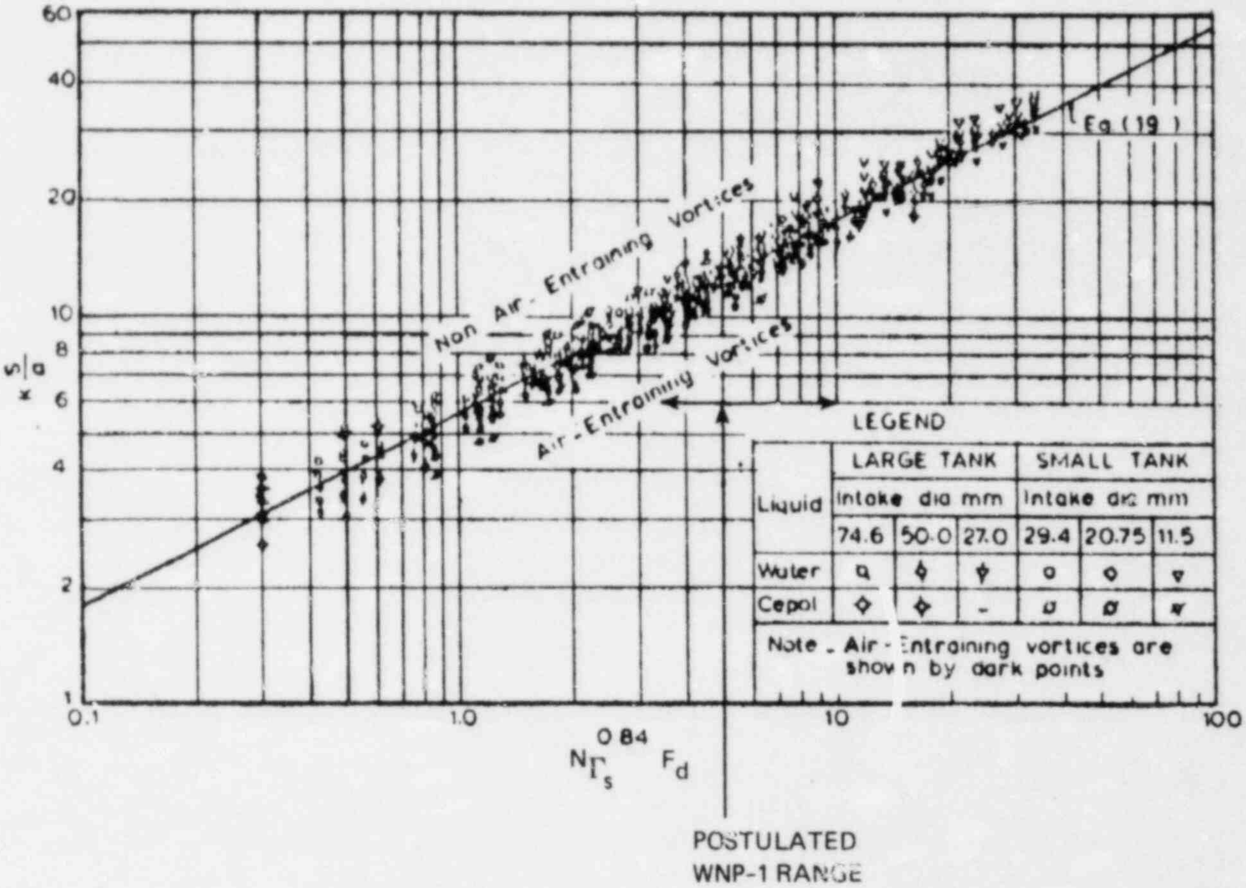


FIGURE 5 CRITERION FOR TYPE OF VORTEX, FROM JAIN et al (7)

Daggett and Keulegan [4] defined a circulation number $(N_{\Gamma})_A$ as $\Gamma A/2Q$, where A is the pipe radius (d/2). Following this definition, for the case of Figures 3A and 3B, $(N_{\Gamma})_A$ will have a value of about 0.43 to 1.5. Referring to Figure 6 reproduced from [4], with s/A of 11.5, the operating range is in the air-core region.

From the above paragraphs, it appears that (without taking credit for suppressing action of sump screens and gratings) a case of maximum circulation generated by up to 75% screen blockage indicates the occurrence of air-core vortices. No information is available in any of the considered publications on the percentage of air that could be drawn into suction pipes nor on the influence of vertical sump screens and gratings on suppressing or weakening air-core vortices.

### 3.1.2 Model Studies on Similar Sumps

The proposed WNP-1 containment sump is a depressed floor sump with screens and gratings and a top solid cover which is always submerged. Similar sumps were found to perform well, as discussed in references [10, 11]. The containment sumps of the Virgil C. Summer Nuclear Power Station and the Bellefonte Nuclear Power Station are very similar to the WNP-1 sumps [16, 17]. These other plants also have single pipe outlet sumps with a common approach flow screen and grating, and a submerged top cover on the sump. Model studies for both the sumps have been performed at ARL, and a report on the former is available [16]. The Seabrook Nuclear Power Station has a two-outlet sump with a solid partition wall separating the sump [18]. Hence, each portion of the Seabrook sump can be considered as a single outlet sump. Model studies of the Seabrook Nuclear Power Station have also been conducted at ARL [18].

Table 3 shows a comparison of important geometric variables, flow variables, and non-dimensional numbers for each of the three sumps; namely, Bellefonte, V.C. Summer, and Seabrook, as compared with the WNP-1 sump. It should be pointed out that the model tests of three sumps involved asymmetrical screen

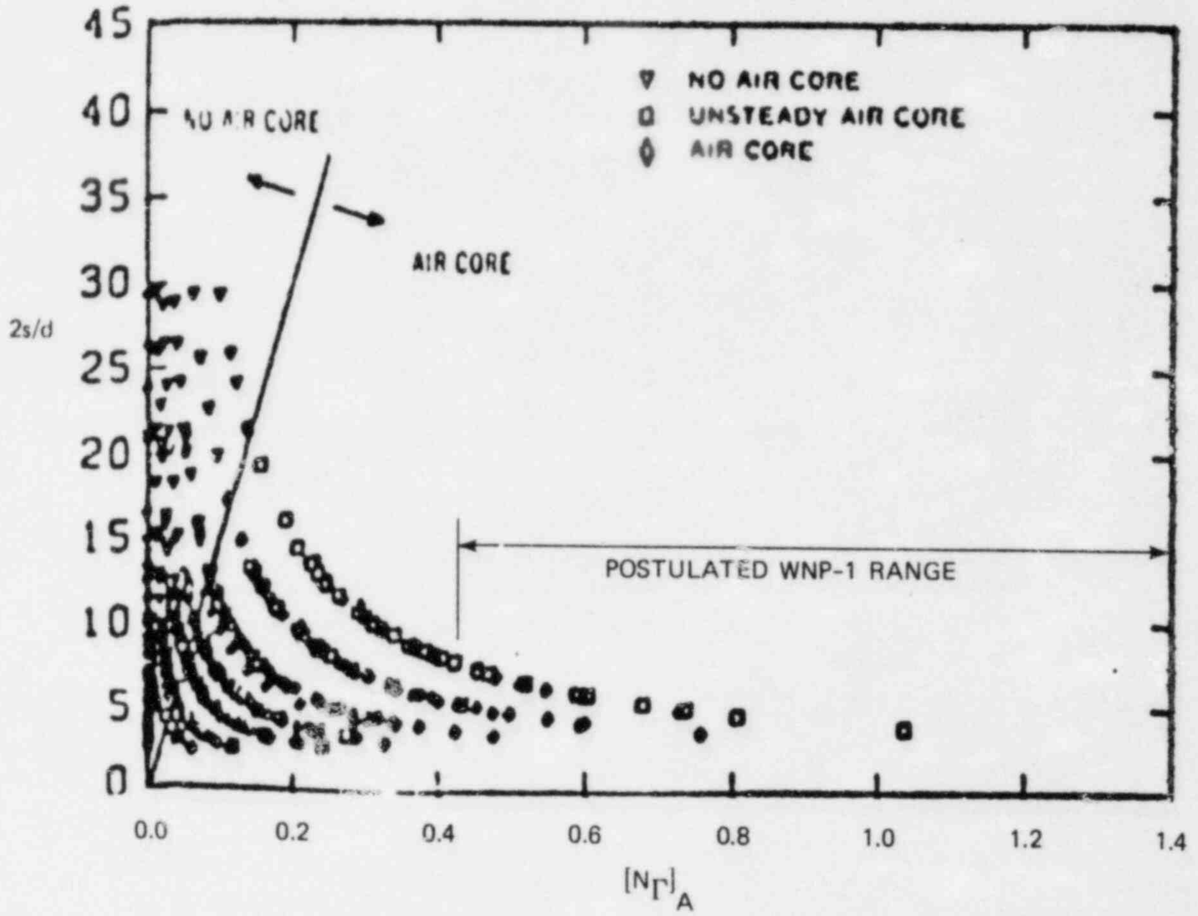


FIGURE 6 REGION OF AIR-CORE FORMATION, FROM DAGGETT AND KEULEGAN (4)

blockages of up to 50%, and operation at higher than Froude velocities, and in the case of the Seabrook sump, higher than normal temperature tests were conducted [16, 17, 18]. Under Item 9 is listed the worst maximum vortex type observed in the model study considering all tests.

It is seen from Table 3 that the Froude number ranges of the WNP-1 sumps are not higher than those for the Bellefonte, V. C. Summer, and Seabrook sumps, and only surface dimples to dye-core vortices may be expected for the WNP-1 sump, based on the comparison using Table 3. It should be pointed out that all the above three sumps used for comparison have submerged top solid covers, similar to the WNP-1 sump.

Table 4 is a listing of typical conditions at which air-entraining vortices occurred based on model studies of other similar containment sumps [19, 20, 21, 22]. Vortex suppressors were subsequently installed for these sumps. In Figure 7, the observed maximum vortex types in various sump models are plotted against the Froude number for cases where data are available for original designs without vortex suppressors. However, for Bellefonte, a vortex suppressor was included in the original design tested at ARL. All data points are taken from corresponding sump model test results [16 to 24], and include cases with or without screen blockages (up to 50%) and tests with higher than Froude scaled velocity. The data for Davis Besse indicate a weak air-core up to the screens. The air-core broke into small bubbles downstream from the screens, and the bubbles were not drawn into the sump, but were found to rise to the surface [22].

By comparison to other sump model test results from Table 4 and Figure 7, no air-drawing vortices are indicated for the WNP-1 range of Froude numbers. This appears logical since the combination of low inlet velocities and relatively high minimum submergence creates more favorable conditions, i.e., lower Froude number and higher s/d values than for most of the other projects used in the comparison. However, an exact prediction of vortexing in WNP-1 sumps using Figure 7 would be difficult.

TABLE 3

Comparison with Similar Sumps

| | Quantity | WNP-1 DHR | WNP-1 CSS | Bellefonte (TVA) | V. C. Summer | Seabrook |
|---|---|---|---|---|---|---|
| 1. | Sump size (length x width x depth), ft (depressed floor only) | 7x6.5 x5 | 7x5.5 x5 | 4 x 5 expanding to 11 x 6; 22' deep | 4 x 4 x 6 | 18 x 9 x 8 |
| 2. | Pipe diameter, d, inch | 20 | 16 | 18 | 12 and 14 | 16 |
| 3. | Flow range, Q, gpm | 6000 | 3000 | 8200 | 3000, 4500 | 3000 to 7850 |
| 4. | Approach flow depth at minimum water level, y, ft | 5.84 | 5.84 | 4 | 10 | 2.5 |
| 5. | Pipe velocity, u, fps | 6.6 | 5.3 | 11.3 | 8.51 and 10.5 | 5.3 to 13.8 |
| 6. | Approach flow velocity, $u_a$, fps (no blockage of screens) maximum average velocity | 0.04 | 0.04 | 0.25 | 10.3 | 0.13 |
| 7. | Submergence above pipe, s, ft | 9.5 to 13.5 | 9.5 to 13.5 | 22.5 | 16 | 8 to 11 |
| 8. | Froude number, $F = u/\sqrt{gs}$ | 0.32 to 0.38 | 0.25 to 0.30 | 0.42 | 0.37 to 0.46 | 0.28 to 0.86 |
| 9. | Maximum observed vortex type | --- | --- | None | 2 | 1 to 3 |
| 10. | Maximum observed swirl angle, degrees | --- | --- | 11.1 | 9.5 | 5.0 |
| 11. | Inlet loss coefficient (average) | --- | --- | 0.32 | 0.30 | 0.37 |
| 12. | Minimum pipe Reynolds number (Re), $ud/\nu \times 10^5$ | 10.6 | 6.7 | 16.9 | 8.5 | 7.0 |
| 13. | Minimum radial Reynolds number ($R_R$), $Q/\nu s \times 10^4$ | 9.9 | 5.0 | 8.1 | 4.1 | 6.0 |
| 14. | Vortex Suppressor | No | No | Yes | No | No |
| 15. | Bell Entrance | Expansion piece | Expansion piece | Curved re-entrant | Yes | Yes |
| 16. | Maximum Screen Blockage, percent, tested | --- | --- | 50 | 50 | 50 |

TABLE 4

Conditions for Air-Entraining Vortices Before Installing Vortex Suppressors With or Without Partially Blocked Screens (from model studies)

| Nuclear Station | Flow gpm/pipe | Submergence ft | Pipe Diameter inch | Froude Number | s/d |
|---|---|---|---|---|---|
| 1. Farley, Unit 1** Intake 1 | 4000 | 3.86 | 14 | 0.75 | 3.50 |
| 2. McGuire* (original design) | 7294 | 1.75 | 18 | 1.2 | 1.22 |
| 3. North Anna* Units 1 and 2 | 3000 | 5.25 | 12 | 0.65 | 5.25 |
| 4. Davis Besse**, Unit 1 | 5500 | 8.0 | 18 | 0.43 | 5.56 |

*without screen blockage
**with screen blockage

3.1.3 Ongoing Containment Sump Reliability Studies (at ARL for DOE and NRC through Sandia National Laboratories)

Numerous rectangular sump configurations with and without flow perturbations, such as screen blockages and streaming approach flow, have been tested at ARL using a full scale facility as a part of a parametric containment sump reliability study [25, 26]. The tested sump configurations included sumps with single outlets as well as with two outlets, and a few tests were conducted with solid partition walls between outlet pipes. Since this research program is not yet complete and no reports are released, no specific results will be mentioned here. However, indications are that the Froude number is a basic parameter in evaluating sumps for vortex susceptibility, and the full scale study showed that the probability for an air-core vortex increases considerably as the Froude number is increased. For the range of Froude numbers of WNP-1 sump (0.28 to 0.38), air-core vortices may be formed, but they would not generate any significant air withdrawals, even without a submerged top cover. With a top cover submerged below minimum water level, any weak air-

NA = NORTH ANNA, UNIT 1
FR = FARLEY, UNITS 1 & 2
MG = McGUIRE
DCC = D.C. COOK
SEA = SEABROOK
VCS = V.C. SUMMER
BF = BELLEFONTE
TMI = THREE MILE ISLAND
DB = DAVIS BESSE

VORTEX TYPE

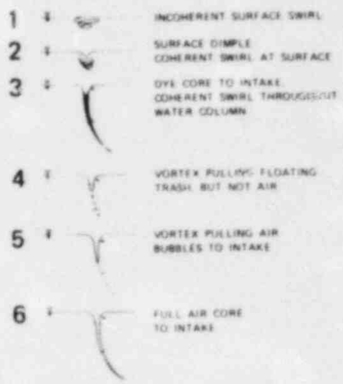


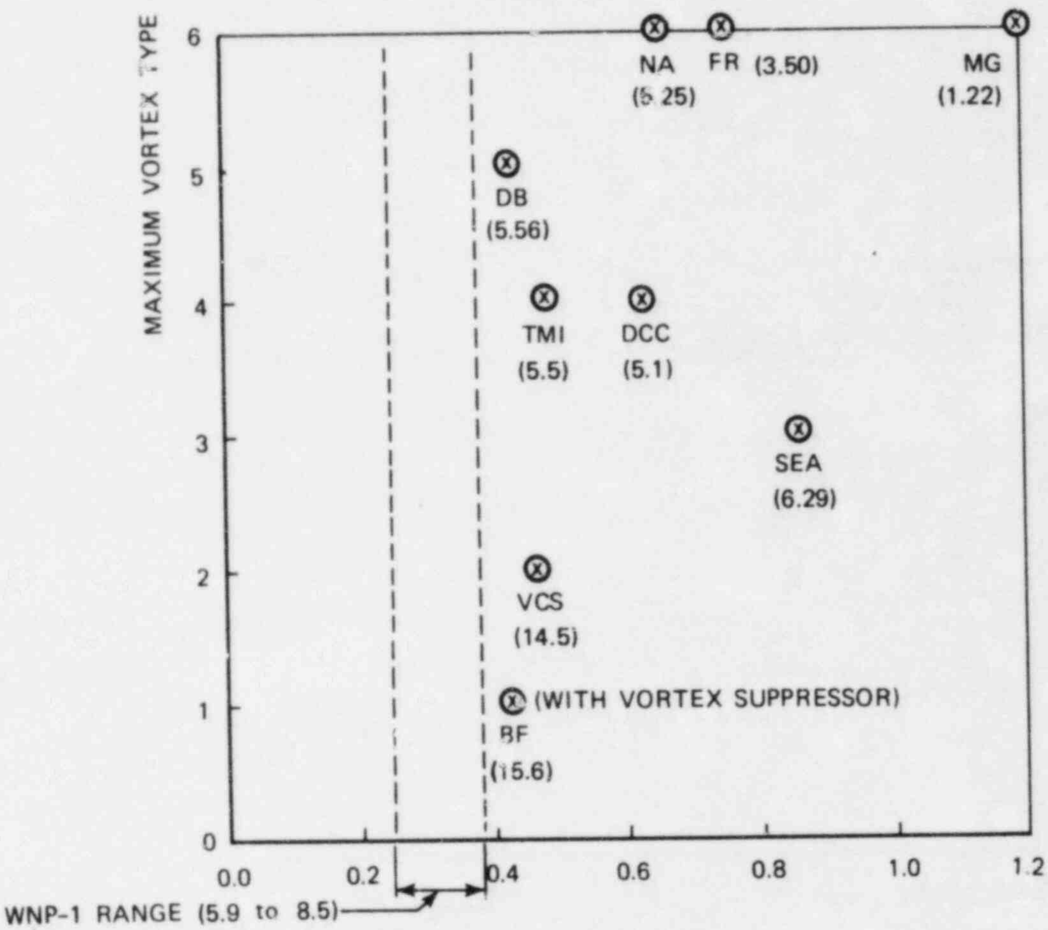


NOTES:

$F = u/\sqrt{gs}$ (DESIGN CONDITIONS)

i) DATA WITH 50% SCREEN BLOCKAGES FOR FR, DB, SEA, DCC, VCS, BF, TMI.

ii) DATA WITH NO SCREEN BLOCKAGES FOR NA AND MG.

iii) s/d VALUES DENOTED IN PARENTHESES.

FIGURE 7 VORTEXING INFORMATION FROM VARIOUS SUMP MODELS (MOSTLY ORIGINAL DESIGNS BEFORE MODIFICATIONS) core vortices outside screens present could be expected to be suppressed by sump screens and gratings. But, unfortunately, sufficient information to guarantee that any air-core vortices will be completely suppressed by these screens and gratings is not available at present. Limited tests with top covers conducted in the full size facility at ARL did not include screen blockage tests. But, the tests with nearly uniform approach flow indicated no coherent core vortices passing through the screen [26].

### 3.1.4 Summary of Vortexing Evaluation

From Sections 3.1.1 through 3.1.3, it may be concluded that under approximately uniform approach flow conditions, no air-drawing vortices are indicated for the WNP-1 sump for its entire ranges of operation. Weak air-core vortices may occur outside the peripheral screens and gratings with partial blockage of sump screens. Insufficient information exists to guarantee that the peripheral screens and gratings themselves will suppress the vortices to the extent that no air will be pulled into pump suction lines.

An acceptable sump performance according to the present regulatory position would be a zero air-withdrawal sump even under flow perturbations such as screen blockages. It seems prudent to investigate the sump performance with a limited hydraulic model study, mainly to verify the suppression by peripheral screens and gratings of any air-core vortices under conditions of partially blocked screens. Remedial measures such as adding vortex suppressors could be derived using the model in the unlikely event of air-withdrawals due to vortices.

## 3.2 Pipe Swirl

Typically, the swirl angles measured in containment sump models (at 2 to 15 pipe diameters from inlet) were found to be less than 10 degrees; generally less than 5 degrees [11]. The higher values are encountered with screen blockages. Since swirl angles are known to decay exponentially with distance along the pipe [27, 28], if the pump is located at a considerable distance from the sump, say 50 or more pipe diameters, the swirl intensities at the pump would be negligible.

A prediction of swirl angles likely to exist in the WNP-1 pipe inlet may be obtained from comparison to similar sumps, as shown in Table 3. Since, in terms of sump size, depth, Froude, and Reynolds number at the range of operation being considered, the closest sump for which data are given in Table 3 is the V.C. Summer sump. This sump and associated flow conditions produced a maximum swirl of about 9.5 degrees at about two pipe diameters from the entrance. The ongoing full size sump studies at ARL indicated, for Froude numbers in the range of 0.3 to 0.4, an upperbound of about 5 degrees for the swirl angle at about 15 pipe diameters from the pipe entrance (equivalent of about 7 degrees at inlet) including perturbations such as screen blockages.

For WNP-1, the DHR and CSS pumps are located at about 165 and 148 ft, respectively, from the sump being connected, mostly by straight pipe length. The expected swirl angles at the pump, assuming an inlet swirl as high as 10 degrees and using a relationship for swirl decay [27], can be calculated by

$$\frac{\tan \theta}{\tan \theta_o} = e^{-\beta \, \Delta x/d}$$

where $\theta$ and $\theta_o$ are the swirl angles at distances $x + \Delta x$ and $x$, respectively, $\beta \simeq 0.02$ from reference 20 with $\Delta x/d \simeq 100$, and $\theta_o \simeq 10$ degrees. Using the above expression, $\theta$ at the pumps will be less than 2 degrees, which presumably is too small to affect the pump performance.

### 3.3 Air-Withdrawal Into Suction Pipes

The evaluation of surface vortexing as described in Sections 3.1.1 and 3.1.3 indicated air-core vortices likely for WNP-1 sump with perturbed approach flows. Based on the ongoing full scale containment sump studies at ARL, any air-withdrawals due to such vortices would be less than 2% (void fraction) for the ranges of Froude numbers of WNP-1 sump. Also, it is quite probable that the sump screens and gratings would weaken or suppress the air-core which would mean zero or near zero air-withdrawals. Since the sump location is outside the shield wall and far away from the likely LOCA locations, no direct impingement of break jets are possible in the sump area to cause any air entrainment due to jet impact. As summarized in Section 3.1.4, a limited model study concentrating on partial screen blockages would be a means of verifying any air-withdrawals and deriving remedial measures towards a zero air-withdrawal sump in the event of finding any air-withdrawals due to vortices.

As regards any air-core submerged vortices, any strong sub-surface vortices to the extent of continuous dissolved air release from the water are unlikely with an available submergence of above 9 ft. Any air release in a subsurface vortex core would amount only to insignificant air-withdrawal rates, as was noted in some instances in the full size sump tests at ARL.

As shown in Figure 2, the top solid cover of the sump is sloping, and hence no air is likely to be trapped underneath the sump cover. Hence, no air withdrawals from trapped air are expected.

### 3.4 Inlet Losses at the Sump

An inlet loss coefficient may be defined as

$$C_L = \frac{\Delta H}{u^2/2g}$$

where

$C_L$ = inlet loss coefficient
$\Delta H$ = total inlet losses including grating and screen losses (in feet of water)

A best estimate of inlet loss coefficient is obtained by comparison to similar sumps for which the inlet loss coefficient has been evaluated by model studies. The sumps of V.C. Summer, Bellefonte, and Seabrook Stations have a bellmouth entrance protruding into the sump [16, 17, 18]. The WNP-1 sump has an expansion piece at the entrance, but has the pipe entrance flush with the wall without any protrusion. The entrance losses for a protruding pipe are known to be higher by as much as 50% compared to non-protruding entrance. From Table 3, it is seen that the inlet loss coefficients, including screen and grating losses for V. C. Summer, Bellefonte, and Seabrook Stations are in the range of 0.3 to 0.37 [16, 17, 18]. For the WNP-1 sump, the inlet loss coefficient could be expected to be in the lower ranges because of a non-protruding inlet, a good estimate of a conservative upperbound value may be about 0.35.

The inlet loss coefficient can also be calculated, accounting for entrance and screen losses, based on available literature. Such a calculation is provided in Appendix A, and the calculated value is 0.35.

The Net Positive Suction Head (NPSH) available to the pump should be calculated allowing for inlet losses with an estimated value of inlet loss coefficient of 0.35, and should be compared to the required NPSH for the pumps. From the data provided by UE&C (Table 1), it is seen that the available NPSH is higher than the required NPSH by about 8 ft and hence, the impact of inlet losses of about a few inches of water may be negligible.

## 4.0 SUMMARY

The following paragraphs summarize the findings of the hydraulic evaluation of the design of the containment recirculation sumps of the Washington Public Power Supply System, Project 1:

1. Based on available literature on basic studies of vortices, and an assumed severely perturbed flow condition at the sump due to asymmetrical screen blockages, it seems that an air core vortex could form. This conclusion may also be reached based on data from the full sized parametric sump study, but air ingestion would not be more than about 2% by volume. However, the vertical sump screens and gratings may suppress or weaken any air core vortices, the sump solid cover being submerged even at the minimum water level. The extent by which the screens and gratings will suppress the vortices is not known definitely. Based on a comparison with other similar sumps, the probability for an air drawing vortex seems slight.

2. The sump is outside the shield wall away from any possible pipe break locations and, as such, no air ingestion or any other problems resulting from high velocity jet impact are to be expected.

3. The top solid cover of the sump is slightly sloping, and would not trap any air, since as the sump fills up, the air will escape.

4. By comparison to results of hydraulic model studies of similar sumps and using the information available from the ongoing full scale tests at ARL, the flow swirl for the inlet pipes may be as high as 10 degrees, especially under asymmetrical screen blockages. Because considerable length of piping, as much as 100 pipe diameters, is available between the sump and recirculation pumps, the pipe swirl will decay to negligible magnitudes near the pumps.

5. Using available literature, the inlet loss coefficient, including entrance and screen losses, is estimated to be about 0.35. Comparison to results of model studies of similar sumps supports this value. Since the available NPSH for the pumps are reported (by UE&C) to be higher than the required NPSH by as much as 8 ft, the impact of the inlet losses on NPSH calculations may be insignificant.

6. In short, a limited hydraulic model study to include the train that could induce the most circulation under partial screen blockages (as shown in Figures 3A and 3B) may be undertaken to verify that any weak air-core vortices, if exist, would be suppressed by the peripheral sump screens and gratings. If any air-withdrawals due to vortices are indicated by the model, remedial measures such as addition of vortex suppressors could be derived from the model study.

REFERENCES

1. Murakami, M., et al., "Flow of Entrained Air in Centrifugal Pumps," 13th Congress, IAHR, Japan, August 31 to September 5, 1969.

2. Patel, B.R., and Runstadler, Jr., P.W., "Investigations into the Two-Phase Flow Behavior of Centrifugal Pumps, Polyphase Flow in Turbomachinery, ASME Winter Annual Meeting, San Francisco, California, December 10-15, 1978.

3. Florjancic, D., "Influence of Gas and Air Admission on the Behavior of Single and Multi-Stage Pumps," Sulzer Research Number, 1970.

4. Daggett, L.L., and Keulegan, G.H., "Similitude Conditions in Free-Surface Vortex Formations," Journal of the Hydraulics Division, ASCE, November 1974.

5. Anwar, H.O., Weller, J.A., and Amphlett, M.B., "Similarity of Free-Vortex at Horizontal Intake," Journal of Hydraulic Research, IAHR 16, No. 2, 1978.

6. Reddy, Y.R., and Pickford, J., "Vortex Suppression in Stilling Pond Overflow," Journal of Hydraulics Division, ASCE, pp. 1685-1697, November 1974.

7. Jain, A.K., Raju, K.G.R., and Garde, R.J., "Vortex Formation at Vertical Pipe Intakes," Journal of Hydraulics Division, ASCE, October 1978, p. 1429-1445.

8. Hattersley, R.T., "Hydraulic Design of Pump Intakes," Journal of the Hydraulics Division, ASCE, pp. 233-249, March 1965.

9. Padmanabhan, M., "Selection and Scaling of Horizontal Gratings for Vortex Suppression," ARL Report No. 62-78, July 1978.

10. Padmanabhan, M., and Hecker, G.E., "Flow Characteristics of Reactor Recirculation Sumps," IAHR, XVIII Congress, Cagliari, Italy, 1979.

11. Nystrom, J.B., Padmanabhan, M., and Hecker, G.E., "Flow Characteristics of Reactor Residual Heat Removal Sumps," Joint Power Generation Conference, ASME/IEEE/ASCE, St. Louis, Missouri, October 1981.

12. Gordon, J.L., "Vortices at Intakes," Water Power, March 1972.

13. Reddy, Y.R., and Pickford, J.A., "Vortices at Intakes in Conventional Sumps," Water Power, March 1972.

14. Prosser, M.J., "The Hydraulic Design of Pump Sumps and Intakes," BHRA Report, July 1977.

15. Dicmas, J.L., and Fornesi, R., "Close Study of Cooling-Tower Pump Intakes," Pumps, Compressors, Valves and Piping, Power Journal, January 1979.

16. Nystrom, J.B., "Model Study of Reactor Containment Sump Flow Characteristics, Virgil C. Summer Nuclear Generating Station," ARL Report No. 47-81, July 1981.

17. Nystrom, J.B., "Hydraulic Model Studies, Bellefonte Nuclear Power Station," ARL Draft Report.

18. Padmanabhan, M., "Investigation of Vortexing and Swirl Within a Containment Recirculation Sump Using a Hydraulic Model, Seabrook Nuclear Power Station," ARL Report No. 25-81, January 1980.

19. "Containment Sump Description and Emergency Core Cooling System Recirculation Mode Test Program," Appendix 6C, Final Safety Analysis Report, J.M. Farley Nuclear Plant Units 1 and 2, 1977.

20. Padmanabhan, M., "Assessment of Flow Characteristics Within a Reactor Containment Recirculation Sump Using a Scale Model," McGuire Nuclear Power Station, ARL Report No. 29-78.

21. Padmanabhan, M., "Hydraulic Model Studies of the Reactor Containment Building Sump, North Anna Nuclear Power Station, Unit 1," ARL Report No. 123-77, July 1977.

22. "Report on the Davis-Besse Nuclear Power Station Unit 1, ECCS Emergency Sump and Pump Suction Line Testing," Final Safety Analysis Report, Davis-Besse Nuclear Station, Unit 1, 1977.

23. Padmanabhan, M., "Hydraulic Model Investigation of Vortexing and Swirl Within a Reactor Containment Recirculation Sump," Donald C. Cook Nuclear Power Station, ARL Report No. 108-78.

24. Durgin, W.W., Neale, L.C., and Churchill, R.L., "Hydrodynamics of Vortex Suppression in the Reactor Building Sump Decay Heat Removal System, Three Mile Island Nuclear Station, Unit 2," ARL Report No. 46-77, February 1977.

25. Durgin, W.W., Padmanabhan, M., Watt, J.J., and Weigand, G.G., "Unresolved Problems Related to the Performance of Containment Recirculation Sumps," 1980 ANS/ENS Topical Meeting, Knoxville, Tennessee, April 1980.

26. Padmanabhan, M., Durgin, W.W., and Weigand, G.G., "Containment Sump Performance - A Parametric Study," ASME/ASCE Joint Mechanics Conference, Boulder, Colorado, June 1981.

27. Padmanabhan, M., and Janik, C.R., "Swirling Flow and Its Effect on Wall Pressure Drop Within Pipes," ASME Winter Annual Meeting, Symposium on Vortex Flows, Chicago, Illinois, November 1980.

28. Wolf, L., *et al.*, "Measurements of the Decay of Swirl in Turbulent Flow," AIAA Journal, May 1969.

29. Weighardt, K.E.G., "On the Resistance of Screens," The Aeronautical Quarterly, Vol. IV, February 1953.

30. Rouse, H., *Engineering Hydraulics*, John Wiley & Sons, 1950.

APPENDIX A

## APPENDIX A

With 75% blocked screens, consider one train of DHR and CSS drawing from the corresponding sumps:

Maximum Flow = 6000 + 3000 = 9000 gpm = 20.1 cfs

Total Area of Screens at Minimum Water Level = 409 $ft^2$

With 75% Blocked Screens, Available Screen Area = 102 $ft^2$

Approach Velocity Upstream of Screens $(u_a) = \frac{20.1}{102} = 0.2$ fps

Diameters of Screen Wires, $d_s = 0.032$ inch

Screen Reynolds Number $= u_a d_s/\nu = 53$

Open Area of Screen $(\beta) = \frac{0.0733^2}{0.1053^2} = 0.485 = 48.5\%$

Referring to Weighardt [29],

$$K = \frac{\Delta p}{\rho u_a^2/2} = \frac{\Delta H_s}{u_a^2/2g} = 6(1 - \beta)\ \beta^{-5/3}\ \left(\frac{u_a d_s}{\nu}\right)^{-1/3}$$

$$= 6 \times 0.515 \times 3.34 \times 0.266 = 2.74$$

or screen loss $\Delta H_s = 2.74 \times \frac{0.2^2}{64.4} = 0.02$ inch

So it is seen that the loss through the screen is negligibly small. Loss through the trashracks will also be negligibly small and is not included.

Referring to Rouse [30], for an entrance with no protrusions,

Entrance Loss Coefficient without any Bell ≃ 0.5

Entrance Loss Coefficient for an Entrance with a Bellmouth ≃ 0.1

From model studies, usually the loss coefficient has been found to increase by as much as 15% due to increased entrance swirl, especially under blocked screen conditions [20].

Since the WNP-1 sump pipe entrances are fitted with an expansion piece, but not a well shaped bellmouth piece, an average value of loss coefficients for the two cases with and without bellmouth which is about 0.3 may be appropriate. Allowing for about 15% increase due to swirl effects caused by screen blockages, a value of $C_L$ equal to 0.35 is estimated.

HYDRAULIC MODEL STUDY OF CONTAINMENT
RECIRCULATION SUMPS

WASHINGTON PUBLIC POWER SUPPLY SYSTEM
(WNP-1)

by
William W. Durgin
John F. Noreika

Prepared for
United Engineers & Constructors, Inc.

George E. Hecker, Director
ALDEN RESEARCH LABORATORY
WORCESTER POLYTECHNIC INSTITUTE
HOLDEN, MASSACHUSETTS

December 1982

## ABSTRACT

A hydraulic model of the Containment Recirculation Sumps of the Washington Public Power Supply System Nuclear Project No. 1 (WNP-1) was constructed at a scale of 1:2.5 in order t evaluate the hydraulic performance in the event of a loss of coolant accident. The Decay Heat Removal (DHR) and Containment Spray System (CSS) would be activated and would withdraw water from the sumps. A series of model tests was conducted under various flowrates, water levels, flow distributions, and screen blockages. Measurements included sump inlet losses, swirl in the pump suction lines, and determination of vortex activity and strength.

Under no circumstances were air-drawing vortices observed. Vortex activity under all test conditions was limited to surface dimples, even under the most severe blockage condition (75 percent blockage). These vortices were located outside the cover plate, and, in general, originated from eddies shed off the support structure.

The maximum swirl angles encountered in the DHR and CSS sump suction lines were 6.61 and 13.5 degrees, respectively. Inlet loss coefficients, representing head losses due to the screens, trashracks, sump and inlet geometry, and the inlet reducer, averaged 0.06 for the DHR and 0.15 for the CSS sump over the range of tests.

The results of the model study in conjunction with the hydraulic evaluation and the literature pertaining to scale effects indicate that the prototype will not experience air entrainment due to free surface vortices. Furthermore, the loss coefficients reported herein can be used in conjunction with pump performance data to evaluate the sufficiency of available net positive suction head (NPSH). Considering the decay of swirl in the outlet lines, even the highest measured values would be reduced to less than 2 degrees over the pipe length. Typically, degradation of pump performance for such small swirl angles is insignificant.

In-plant pre-operational testing of the containment sumps would be unlikely to add significantly to the findings presented herein. In fact, due to the difficulty of conducting such tests and associated measurements, it is likely that they would be less conclusive.

# TABLE OF CONTENTS

# INTRODUCTION

In the Washington Public Power Supply System Nuclear Project No. 1 (WNP-1), the Emergency Core Cooling System (ECCS) is designed to cool the reactor core and the Containment Spray System (CSS) is designed to reduce the Containment pressure and temperature following a Loss of Coolant Accident (LOCA). The Decay Heat Removal (DHR) System, which is part of the ECCS and the Containment Spray System would be activated and draw water from the Borated Water Storage Tank (BWST) during the initial phase. When the BWST water level reaches a predetermined setpoint, these systems are switched to the recirculation mode, wherein water is withdrawn from the Containment recirculation sumps. Both the DHR and CSS pumps may be required to operate in this mode for extended periods of time in order to provide sufficient heat removal. It is necessary that, in the recirculation mode, no flow conditions develop that could adversely affect the hydraulic performance of the ECCS system. Formation of air entraining vortices should be prevented to ensure satisfactory pump performance. In addition, intake losses and swirl angles should be small enough such that the required NPSH of the pumps is satisfied and the pre-rotation at the pump inlets due to the intake swirl is minimal.

A hydraulic model of the Washington Public Power Supply System Nuclear Project No. 1 containment recirculation sumps was tested at the Alden Research Laboratory (ARL). The objectives of the study were to investigate flow conditions which could lead to air entraining vortices, high swirl angles, and high inlet losses which could affect the performance of the decay heat removal (DHR) and containment spray system (CSS) pumps. Operating conditions included appropriate ranges of water levels, flowrates, flow distributions, and screen blockages.

This report includes a description of the methodology as well as results and interpretation of the results for evaluation of sump performance.

# PRELIMINARY INVESTIGATION

A detailed hydraulic evaluation of the design of the containment recirculation sumps of WNP-1 and the proposed model study was conducted at ARL prior to implementation of the model study. The report, "Hydraulic Evaluation of the Design of Containment Recirculation Sumps Washington Public Power Supply System Nuclear Project 1 (WNP-1)," is bound as a companion to this report.

Subsequent to the completion of the hydraulic evaluation, a proposal was made that outlined the objectives and criteria needed for construction and evaluation of a hydraulic model. A test procedure was developed and implemented in the model study in order to identify conditions which would cause unacceptable performance of the containment sumps. A limited model was proposed in order to study one sump train to establish hydraulic performance. If performance was unacceptable, the second sump train would have been modeled.

In the first report, existing literature and results of sump studies conducted at ARL and elsewhere were used to perform an evaluation of the containment recirculation sump of WNP-1. The sumps were evaluated in terms of vortex formation, swirl, and inlet losses. Major results from the evaluation are summarized as follows: 1) air drawing vortices will not occur under any blockage arrangement due to suppression of vortices from screens and trashracks; however, suppression of vortices cannot be predicted with certainty; 2) swirl may occur up to ten degrees at the pipe inlet but will decay to less than two degrees at the recirculation pumps, and 3) loss coefficients may range up to 0.35 but would not have any significant impact. It was concluded that a limited model study was necessary in order to verify that any weak air-core vortices would be suppressed by sump screens and grating system.

## PROTOTYPE DESCRIPTION

The reactor containment building of WNP-1 contains recirculation sumps located between the shield wall and containment outer wall. Figure 1 shows the southwest quadrant and indicates the 50 degree arc section simulated in this study. The test section contains a DHR sump located at 235 degrees on center and a CSS sump located at 245 degrees on center. Each sump has a centerline radius of 68 ft and each is 7 ft wide. The sumps are recessed into the floor elevation at 405 ft.

Both sumps have sloping floors of approximately 4.5 degrees with a minimum elevation of 399 ft 1 inch for the DHR sump and 399 ft 5 inches for the CSS sump, Figure 2. The DHR sump is 7 ft x 6.5 ft and contains a 20 inch suction pipe with centerline at elevation 401 ft 5 inches. The inlet of the suction line is flush with the outer wall of the sump and is equipped with an 11 inch long, 26 inch x 19.25 inch ID conical reducer. The CSS sump is 7 ft x 5.5 ft and contains a 16 inch diameter suction line whose centerline is at elevation 401 ft 3 inches. The inlet is also flush with the wall and is equipped with a 10 inch long, 21 inch x 15.25 inch ID conical reducer.

An 8 inch wide x 4 inch high curb, with radii at 63 ft 10 inches and 71 ft 6 inches and encompassing an arc of 36.5 degrees, serves as a support for a fine mesh screen, screen frame, and trashrack 4 ft 4 inches high. The screen and trashrack are covered by a one inch thick deck plate which slopes inward at a slope of 1/16 inch per ft to a minimum elevation of 409 ft 11 1/2 inches, Figure 3. The solid deck plate will be submerged at the minimum water level of 410.84 ft. The deck plate will have a row of 1/2 inch diameter vent holes on 12 inch centers located on the high side of the plate approximately 2 inches from the edge of the I-beam frame.

The maximum flowrate through the CSS and DHR suction lines are 3000 and 6000 gpm per pipe, respectively. Water elevation varies from 410.84 ft to a maximum of 415 ft, which provides a minimum pipe submergence of about 9.5 ft.

Temperature of the water in the containment building could vary from 255°F to 55°F. All pertinent data, relative to the sump, supplied by UE&C, are summarized in Table 1.

TABLE 1

WNP-1
Containment Sump Data

Sump Water

Water Levels - Maximum EL 415.00 ft
- Minimum EL 410.84 ft

Water Temperature - Maximum 255°F
- Minimum 55°F

pH - 8.3 to 9.3

| Sumps | DHR | CSS |
|---|---|---|
| Number | 2 | 2 |
| Size (approx.) | 7' x 6'6" x 5' (depth) | 7' x 5'6" x 5' (depth) |
| Bottom EL (minimum) | EL 399'-1" | EL 399'-5" |
| Suction Pipe Diameter | 20" | 16" |
| Centerline Elevation | EL 401'-5" | EL 401'-3" |

| Trashracks and Screens | Trashrack | Screen |
|---|---|---|
| Material | A-36 Steel | Stainless Steel Series 300 |
| Overall Size, Trashrack<br>Bar Spacing | See Drawing<br>No. 9779-F-101378 | |
| Mesh | Mesh per linear inch = 9 1/2<br>Diameter of wire = 0.032"<br>Width of opening = 0.0733" | |
| Solid Deck Plate | 1" thick stainless steel<br>EL of top of deck = EL 409' 11 1/2" (minimum) | |

TABLE 1 (continued)

WNP-1

Containment Sump Data

| Trashracks and Screens | Trashrack | Screen |
|---|---|---|
| Vent Holes | One row of 1/2" diameter holes through deck at high point, 2" from edge of I-Beam frame, on 12" centers | |
| **Pumps** | **DHR** | **CSS** |
| Number | 2 (1 per train) | 2 (1 per train) |
| Type | Horizontal Single Stage | Horizontal Single Stage |
| Location | Gen'l Serv. Bldg. EL 385' | Gen'l Serv. Bldg. EL 385' |
| Capacity | 5,125 gpm at 385'<br>6,375 gpm at 270' | 3,000 gpm at 530'<br>7,400 gpm at 370' |
| Maximum Possible Flow Under Recirculation Mode | 6,000 gpm | 3,000 gpm |
| Design Temperature | 350°F | 300°F |
| Operating Temperature | | |
| Maximum | 305°F | 255°F |
| Minimum | 55°F | 55°F |
| NPSH Required at Centerline of Impeller | 14' at 5,125 gpm | 12' at 3,000 gpm |
| NPSH Available at Centerline of Impeller | 23.5' at 6,000 gpm | 20' at 3,000 gpm |
| | (per UE&C prior to this evaluation) | |

## INVESTIGATION OF FLOW CONDITIONS

Poor pump performance can be attributed to common adverse flow conditions which were investigated in the model study.

1. Entrained Air - One of the major contributors to reduced pump performance, air entrainment can be due to air entraining vortices at or in the vicinity of the sump, entrapped air suctioned off the bottom of the cover plate, or from outgassing caused by low pressures associated with submerged vortices. Air entrainment can also occur due to impingement of breakflow jets. However, this is not applicable in the present investigation as the sumps are located outside the shield wall and are not exposed to any breakflow jets. Concentrations of air of approximately three percent in suction lines have been shown to cause serious reductions of pump performance (1).

2. Swirling Flow - Dependent on vortex activity, approach flow patterns, and screen blockage, swirling flow can be established in the suction lines. Large swirl is undesirable as it could affect intake losses which would lessen the available NPSH for pumps or induce pre-rotation in the pump inlet when the connecting pipes are short.

3. Inlet Losses - Intake losses caused by screens, entrance conditions, or swirling flow, may lead to insufficient NPSH at pump suctions. Since inlet losses can be difficult to predict, model tests are often used for direct measurement. Head losses caused by the screens, trashracks, sump and inlet geometry, including the inlet reducer, are included in the loss coefficients for both sumps. Suction pipe line entrance losses are not included.

## SIMILITUDE

The study of dynamically similar fluid motions forms the basis for the design of models and the interpretation of experimental data. The basic concept of dynamic similarity may be stated as the requirement that two systems with geometrically similar boundaries have geometrically similar flow patterns at corresponding instants of time (2). Thus, all individual forces acting on corresponding fluid elements of mass must have the same ratios in the two systems.

The condition required for complete similitude may be developed from Newton's second law of motion:

$$F_i = F_p + F_g + F_v + F_t \qquad [1]$$

where

$F_i$ = inertia force, defined as mass, M, times the acceleration, a
$F_p$ = pressure force connected with or resulting from the motion
$F_g$ = gravitational force
$F_v$ = viscous force
$F_t$ = force due to surface tension

Additional forces may be relevant under special circumstances, such as fluid compression, magnetic or Coriolis forces, but these had no influence on this study and were, therefore, not considered in the following development.

Two systems which are geometrically similar are dynamically similar if both satisfy the dimensionless form of the equation of motion. Equation [1] can be made dimensionless by dividing all the terms by $F_i$. Rewriting each of the forces of Equation [1] as:

$F_p$ = net pressure x area = $\alpha_1 \Delta p L^2$

$F_g$ = specific weight x volume = $\alpha_2 \gamma L^3$

$F_v$ = shear stress x area = $\alpha_3 \mu \Delta u/\Delta y$ x area = $\alpha_3 \mu u L$

$F_t$ = surface tension x length = $\alpha_4 \sigma L$

$F_i$ = density x volume x acceleration = $\alpha_5 \rho L^3 u^2/L = \alpha_5 \rho u^2 L^2$

where

$\alpha_1$, $\alpha_2$, etc. = proportionality factors

L = representative linear dimension

p = net pressure

$\gamma$ = specific weight

$\mu$ = dynamic viscosity

$\sigma$ = surface tension

$\rho$ = density

u = representative velocity

Substituting the above terms in Equation [1] and making it dimensionless by dividing by the inertial force, $F_i$, we obtain:

$$\frac{\alpha_1}{\alpha_5} E^{-2} + \frac{\alpha_2}{\alpha_5} F^{-2} + \frac{\alpha_3}{\alpha_5} R^{-1} + \frac{\alpha_4}{\alpha_5} W^{-2} = 1 \qquad [2]$$

where

$E = \frac{u}{\sqrt{\Delta p/\rho}}$ = Euler number; $\frac{\text{Inertia Force}}{\text{Pressure Force}}$

$F = \frac{u}{\sqrt{gL}}$ = Froude Number; $\frac{\text{Inertia Force}}{\text{Gravity Force}}$

$$R = \frac{u\,L}{\mu/\rho} \quad = \text{Reynolds number;} \quad \frac{\text{Inertia Force}}{\text{Viscous Force}}$$

$$W = \frac{u}{\sqrt{\sigma/\rho L}} \quad = \text{Weber number;} \quad \frac{\text{Inertia Force}}{\text{Surface Tension Force}}$$

Since the proportionality factors, $\alpha_1$, are the same in model and prototype, complete dynamic similarity is achieved if all the dimensionless groups, E, F, R, and W, have the same values in model and prototype. In practice, this is difficult to achieve. For example, to have the values of F and R the same requires either a 1:1 "model" or a fluid of very low kinematic viscosity in the reduced scale model. Hence, the accepted approach is to select the predominant force and then design the model to the appropriate dimensionless group. The influence of the other forces would be secondary and are called scale effects (2, 3).

## Froude Scaling

Models involving a free surface are constructed and operated using Froude similarity since the flow process is controlled by gravity and inertia forces. The Froude number representing the ratio of inertia to gravitational force:

$$F = U/\sqrt{gs} \qquad [3]$$

where

- $U$ = average velocity in the pipe
- $g$ = gravitational acceleration
- $s$ = submergence, the representative linear dimension

was, therefore, made equal in model and prototype:

$$F_r = F_m/F_p = 1 \qquad [4]$$

where

r = ratio

m = model

p = prototype

In modeling of an intake sump to study the formation of vortices, it is important to select a reasonably large geometric scale to achieve large Reynolds numbers and to reproduce the curved flow pattern in the vicinity of the intake (4). At sufficiently high Reynolds numbers, an asymptotic behavior of energy loss coefficients with Reynolds number is usually observed (3). Hence, with $F_r = 1$, the basic Froudian scaling criterion, the Euler numbers, E, will be equal in model and prototype. This implies that flow patterns and loss coefficients are equal in model and prototype at sufficiently high Reynolds numbers. A geometric scale of $L_r = L_m/L_p = 1/2.50$ was chosen for the model, where L, refers to length. From Equations [3] and [4], using $s_r = L_r$, the velocity, discharge, and time scales were:

$$U_r = L_r^{0.5} = 1/\sqrt{2.50} = 1/1.58 \qquad [5]$$

$$Q_r = L_r^2\, U_r = L_r^{2.5} = 1/(2.50)^{2.5} = 1/9.88 \qquad [6]$$

$$t = L^{0.5} = 1/\sqrt{2.50} = 1/1.58 \qquad [7]$$

Similarity of Vortex Motions

Fluid motions involving vortex formation in sumps of low head pump intakes have been studied by several investigators (5, 6, 7, 8).

Viscous and surface tension forces could influence the formation and strength of vortices (5, 6). The relative magnitude of these forces on the fluid inertia force is reflected in the Reynolds and Weber numbers, respectively, which are defined as:

$$R = u\ d/\nu \qquad [8]$$

$$W = \frac{u}{(\sigma/\rho r)^{1/2}} \qquad [9]$$

where $\nu$ = kinematic viscosity of the fluid, r = characteristic radius of vortex and d = intake diameter. It was important for this study to ascertain any deviations in similitude attributable to viscous and surface tension forces in the interpretation of model results. For large R and W, the effects of viscous and surface tension forces are minimal, i.e., inertial forces predominate. Surface tension effects are negligible when r is large, which will be true for weak vortices where the free surface is essentially flat. Conversely, only strong air-core vortices are subject to surface tension scale effects. Moreover, an investigation using liquids of the same viscosity but different surface tension coefficients ($\sigma = 4.9 \times 10^3$ lb/ft to $1.6 \times 10^3$ lb/ft showed practically no effect of surface tension forces on both weak and strong vortex flow (5). The vortex severity, S, is therefore, mainly a function of the Froude number, but could also be influenced by the Reynolds number.

$$S = S\ (F,\ R) \qquad [10]$$

Anwar (4) has shown by principles of dimensional analysis that the dynamic similarity of fluid motion in an intake is governed by the dimensionless parameters given by:

$$\frac{4Q}{u_\theta\ d^2}\ ,\ \frac{u}{\sqrt{2gs}}\ ,\ \frac{Q}{\nu\ s}\ \text{and}\ \frac{d}{2s}$$

where

$Q$ = discharge through the outlet

$u_\theta$ = tangential velocity at a radius equal to that of outlet pipe

$d$ = diameter of the outlet pipe

Surface tension effects were neglected in his analysis, being negligible for weak vortices. The influence of viscous effects was defined by the parameter $Q/(\nu\ s)$, known as a radial Reynolds number, $R_R$.

For similarity between the dimensions of a vortex of strengths up to and including a narrow air-core type, it was shown that the influence of $R_R$ becomes negligible if $Q/(\nu\ s)$ was close to or greater than $3 \times 10^4$ (4). As strong air-core type vortices, if present in the model, would have to be eliminated by modified sump design, the main concern for interpretation of prototype performance based on the model performance would be on the similarity of weaker vortices, such as surface dimples and dye-cores. For the chosen scale, $R_R$ for the two sumps, over the chosen range of flows, varies from $1.4 \times 10^4$ to $2.4 \times 10^4$ for the CSS sump and $2.8 \times 10^4$ to $4.8 \times 10^4$ for the DHR sump. Since this is close to and exceeding the accepted value in the literature, viscous forces would have a secondary role in the model study. Dynamic similarity is obtained by equalizing the parameters $4Q/u_\theta d^2$, $u/\sqrt{2gs}$, and $d/2s$ in model and prototype. A Froude model would satisfy this condition.

To compensate for any possible excessive viscous energy dissipation and, consequently, less intense model vortex, various investigators have proposed increasing the model flow and, therefore, the approach and intake velocity, since the submergence is maintained constant. Operating the model at the prototype inlet velocity (pipe velocity) is believed by some researchers to achieve the desired results (5). This is often referred to as equal velocity rule, and is considered to give conservative predictions of prototype performance. The test procedure for the present study incorporated testing the model at prototype pipe velocities to achieve conservative predictions.

## Dynamic Similarity of Flow Through Screens

In addition to providing protection from debris, screens tend to suppress non-uniformities of the approach flow. The aspects of flow through screens of concern in a model study are: (1) energy loss of fluid passing through the screen; (2) modification of velocity profile and the deflection of streamlines at the screen; and (3) production of turbulence. As all these factors could affect vortex formation in a sump with approach flow directed through screens, a proper modeling of screen parameters is important.

The loss of energy across the screen occurs at a rate proportional to the drop in pressure, and this loss dictates the effectiveness of the screen in altering velocity profiles. The pressure drop across the screen is analogous to the drag induced by a row of cylinders in a flow field and could be expressed in terms of a pressure-drop coefficient K (or alternately a drag coefficient), defined as (9):

$$K = \frac{\Delta p}{1/2\ \rho\ U^2} = \frac{\Delta H}{U^2/2g} \qquad [11]$$

where

$\Delta p$ = drop in pressure across the screen
$U$ = mean velocity of approach flow
$\rho$ = density of the fluid
$\Delta H$ = head across the screen
$g$ = acceleration due to gravity

From the available literature on the topic (9, 10, 11, 12), it may be seen that

$$K = f(R_s, S', \text{Pattern}) \qquad [12]$$

where

$R_s$ = screen Reynolds number, $U\,d_w/\nu$, $d_w$ being the wire diameter of the screen

$S'$ = solidity ratio equal to the ratio of closed area to total area of screen

Pattern = geometry of the wire screen

If the solidity ratio and the wire mesh pattern are the same in the model and prototype screens, the corresponding values of K would only be a function of the screen Reynolds number. This is analogous to the coefficient of drag in the case of the circular cylinder. It is known that K becomes practically independent of $R_s$ at values of $R_s$ greater than about 1000 (9, 10). However, for models with low approach flow velocity and with fine wire screens, it is necessary to ascertain the influence of $R_s$ on K for both the model and prototype screens before selecting screens for the model which are to scale changes in velocity distribution.

Velocity modification equations relating the upstream velocity profile and downstream velocity profile have been derived based on different theories (9). Most of these indicate a linear relationship between upstream velocity profile and downstream velocity profile, shape and solidity ratio of screen, and value of K. If the wire shape and solidity ratios are the same in the model and prototype screens, it is possible to select a suitable wire diameter to keep the values of K approximately the same for the model and prototype screens at the corresponding Reynolds number ranges. Identical velocity modifications would be produced by the respective screens if the loss coefficients were identical.

The pressure loss coefficient to Reynolds number relationship of fine screens has been investigated at ARL (13). Based on the similarity of pressure loss and velocity modifications, screen dimensionally equal to the prototype screen was used in the model. Since the model screen Reynolds number was about 63 percent that of the prototype for Froude scale velocity, the loss coefficient was sufficiently high to simulate head losses adequately and, therefore, velocity profile modifications. In any case, screen blockages cause changes in velocity distributions far outweighing changes due to screen.

## Scale Effects

Generic containment sump reliability studies (18) have experimentally determined the reliability of model studies in predicting the hydraulic performance of prototype containment sumps. The program, for models in the 1:2 to 1:4 range, concluded that no scale effects were evident in the prediction of average vortex types and persistence. Swirl angles showed no scale effects if the model $R_a$ (approach flow Reynolds number) was greater than $3.0 \times 10^4$. Swirl angles were found to average six degrees without screen blockage and up to 12.5 degrees with screen blockage. If model pipe Reynolds numbers ($R_e$) are maintained above $1.0 \times 10^5$, then the inlet loss coefficients likewise are not affected by scale effects.

Minimum values for the WPS model $R_a$ are $2.1 \times 10^4$ and $3.6 \times 10^4$ for the CSS and DHR sump, respectively, and the minimum model $R_e$ are $1.62 \times 10^5$ and $2.43 \times 10^5$ for the two sumps. Based on the criteria established in the literature (18), the model $R_a$ and $R_e$ essentially met or exceeded the minimum values. It can be concluded, therefore, that the model was independent of scale effects for vortex, swirl and inlet loss coefficient measurements under Froude scale conditions. Test runs under the equal velocity rule were included as a conservative measure.

## MODEL DESCRIPTION

The model was constructed in an elevated steel tank at a scale ratio of 1:2.5. Model boundaries were as indicated in Figure 1 and were chosen to allow for sufficient flow pattern control. Water was pumped from a storage sump and supplied to the steel tank outside of the test section through a perforated plate diffuser. The water subsequently entered the test section through 1/8 inch perforated plate flow straighteners. The water level was maintained by an inlet control valve and a 10 inch adjustable overflow pipe. Figure 4 shows the general arrangement of the model.

The curved model walls corresponding to containment and the shield wall were constructed of wood to form the proper radius. Each sump was constructed of Lucite to allow visual monitoring of flow patterns and vortex activity. The simulated structural supports were constructed using combinations of PVC and wood. The cover plate was made of Lucite to enable monitoring of vortices and trapped air. The screen panels were fabricated using 0.032 inch wire mesh, eight per inch, while the trash grates were 9/16 inch x 9/16 inch x 9/16 inch plastic louvered egg grates (Figures 5 and 6).

The suction pipes were steel, six and eight inch schedule 40, and sump outlet reducers were fabricated out of Lucite. Each suction pipe test section contained a vortimeter for swirl measurements, ten pairs of piezometer taps for pressure gradient measurements, an ASME orifice flowmeter, and a control valve (Figure 7). Piezometer taps and orifice meters were connected to air-water manometer boards (Figure 8). The vortimeters were connected to mechanical rotation counters.

# INSTRUMENTATION AND OBSERVATION TECHNIQUES

## Flow Measurements

Flowrates in each suction line were controlled by butterfly valves, located downstream of the test sections, and were measured using orifice meters. Orifice meters and coefficients were standard ASME design and air-water manometers were used for differential pressure measurements.

## Pressure Gradients

Each suction line contained ten pairs of piezometer taps. Each pair was connected to a differential air-water column on a manometer board with the sump water level as a reference pressure. During each test, documentation of the differential pressures were made by photographing the manometer board as shown in Figure 9. The inlet losses ($\Delta H_I$) were calculated from the pipeline hydraulic gradient measured in each test and included losses due to the screens, trashracks, inlet and sump geometry, and inlet reducers. The loss was measured by extrapolating the pipeline hydraulic gradient to the conical reducer outlet by use of a least squares fit (linear regression analysis) after adjusting for the loss due to the vortimeters (Figure 10). Inlet loss coefficients were then computed by subtracting the extrapolated head at inlet reducer ($\Delta H_I$) from the total head in the sump and a loss coefficient defined as:

$$K = \frac{\Delta H_I - U^2/2g}{U^2/2g} \qquad [13]$$

where

K = loss coefficient

U = average velocity

$\Delta H_I$ = adjusted inlet loss

and $U^2/2g$ represents the calculated velocity head in the pipe .

Pipe Swirl

Average swirl measurements for each suction line was measured by a crossed-vane vortimeter. Rotations were averaged over a 30-second interval by a counting device and rotational direction recorded.

Average swirl angles are defined as the arctangent of the maximum tangential velocity divided by axial velocity. The maximum tangential velocity is the rotational speed times the pipe circumference and the average swirl angle is defined by

$$\theta = \arctan \frac{\pi d N}{U} \qquad [14]$$

where

N = revolutions per second
d = pipe diameter, ft
U = mean axial velocity, ft/sec

Flow Patterns and Vortex Activity

Visual aids, such as dye and slightly buoyant paper balls, were used to identify flow patterns and vortex activity. Vortex strength was determined by using a scale of 1 to 6 (Figure 11). Through observation, the strength of vortices were determined according to this scale. Photographic documentation of adverse flow patterns or vortices was obtained as appropriate.

## TEST PROCEDURE

Model operation was initiated by filling the model tank to a predetermined level which was maintained by an overflow pipe. All manometer lines were then purged of air and checked visually. Flowrates were set by regulating the downstream control valve and measuring the orifice meter deflections. Once water level and flowrates were set, 20 minutes were allowed for the model to reach equilibrium.

Each test proceeded for 20 minutes after equilibrium was established. All measurements made were recorded on data sheets and included:

a) three gradeline photographs at time 0, 10, and 20 minutes
b) vortex strength recorded every 30 seconds
c) vortimeter rotations and direction every 30 seconds

Vortimeter and vortex data were recorded simultaneously for each test in case correlation was necessary. All tests were run at normal ambient laboratory water temperature which varied from 58°F to 63°F.

# TEST PROGRAM

The test program was designed to establish the combination of flow distribution and screen blockage which produced the poorest hydraulic sump performance. Two initial tests were run (WPS-1, 2) at low water level, without screen or distributor blockage to establish baseline performance at Froude scale and Equal Velocity Rule conditions. Tests were then run at Froude scale velocities and at low water level to determine sump performance for various flow distributions, and screen blockage schemes using 50 percent screen blockage (WPS 3-10). Two blockage schemes from Tests WPS 3-10 were then selected and the nominal screen blockage increased from 50 to 75 percent (Tests WPS 11-18). These tests were run at both high and low water levels and at Froude scale and Equal Velocity Rule conditions. Tables 2 and 3 summarize the test program and define the parameters that were varied in each test. Blockage schemes are defined in Figures (12, 13, 14).

Survey tests with the DHR sump operating independently were conducted under the various flow, water level and blockage parameters. The two worst operating conditions were chosen and fully documented (Tests WPS 20 and 21). Test summaries are located in Tables 2 and 3.

TABLE 2

TEST PROGRAM

| Test Name | Water Elevation | Flowrate | Flow Distribution | Screen Blockage |
|---|---|---|---|---|
| WPS-1 | E1 | F1 | H0 | S0 |
| WPS-2 | E1 | F2 | H0 | S0 |
| WPS-3 | E1 | F1 | H1 | S0 |
| WPS-4 | E1 | F1 | H2 | S0 |
| WPS-5 | E1 | F1 | H3 | S0 |
| WPS-6 | E1 | F1 | H3 | S1 at 50% |
| WPS-7 | E1 | F1 | H3 | S2 at 50% |
| WPS-8 | E1 | F1 | H3 | S3 at 50% |
| WPS-9 | E1 | F1 | H3 | S4 at 50% |
| WPS-10 | E1 | F1 | H3 | S5 at 50% |
| WPS-11 | E1 | F1 | H3 | S4 at 75% |
| WPS-12 | E1 | F1 | H3 | S5 at 75% |
| WPS-13 | E2 | F1 | H3 | S4 at 75% |
| WPS-14 | E2 | F2 | H3 | S4 at 75% |
| WPS-15 | E2 | F1 | H3 | S5 at 75% |
| WPS-16 | E2 | F2 | H3 | S5 at 75% |
| WPS-17 | E1 | F2 | H3 | S4 at 75% |
| WPS-18 | E1 | F2 | H3 | S5 at 75% |
| WPS-20 | E1 | F2 | H3 | S3 at 50% |
| WPS-21 | E1 | F2 | H3 | S4 at 50% |

NOTE: Tests WPS-1 thru WPS-18 were conducted with both DHR and CSS pipes operating.
Tests WPS-20 and WPS-21 were conducted with only the DHR pipe operating.

TABLE 3

TEST PARAMETER DEFINITIONS

| Flowrates: | (DHR) | (CSS) | |
|---|---|---|---|
| F1 | 1.38 cfs | 0.68 cfs | Froude Scale |
| F2 | 2.34 cfs | 1.06 cfs | Equal Velocity Rule |

Water Elevations:

E1 corresponding to EL 410.28 ft

E2 corresponding to EL 415.00 ft

Flow Distribution

H0 No Blockage

H1, H2, H3 Defined on Figure 12

Screen Blockage

S0 No Blockage

S1, S2, S3, S4, S5 50% Screen Blockage Schemes as Defined on Figure 13

S4, S5 75% Screen Blockage Schemes as Defined on Figure 14

## TEST RESULTS

Initial Tests (WPS 1-2) established a baseline for evaluation of flow distributor and screen blockage schemes. Flow distributor blockage schemes were tested in WPS 3-5. Blockage H3 was chosen as a result of the high persistence of a type 2 vortex and larger swirl angles than the H2 blockage which also indicated the same persistence of type 2 vortices. H1 was not chosen despite the relatively higher loss coefficient in the CSS sump because of the lack of vortex activity. Screen blockage schemes (Tests 6-10) were conducted with the H3 flow distributor blockage. S4 and S5 schemes (Tests WPS 9-10) were the only blockages which induced a type 2 vortex 100 percent of the time. Nominal 75 percent blockage tests (Tests WPS 11-18) were conducted with these blockage schemes. Under one-sump operation, survey tests with 50 percent blockage, schemes S3 and S4, produced the worst vortex activity. Tests were conducted (WPS-20 and WPS-21) under these conditions with only the DHR sump operational. Test results are shown in Table 4 and include maximum vortex type and persistence, swirl angles, and inlet head losses and loss coefficients.

Under all tests conducted at low water, (Tests 1-12, 17, 18), vortex activity was limited to types 1 and 2. The worst vortices were incoherent, short lived and shifting, forming from eddies shed from the screens and grates outside the sump cover plate, Figures 15 and 16. Vortices, in general, were located outside the screens and grates between the sump train splitter wall and the DHR sump. At high water with maximum screen blockage (Tests 13-16), the maximum vortex was a type 2 even under the Equal Velocity Rule. Air was not observed to be trapped under the cover plate as the vent holes provide sufficient relief. The vortex results of all tests are shown in Table 4.

Swirl measurements calculated from vortimeter rotation rates were obtained for both the CSS and DHR suction lines. The maximum swirl angle for the DHR line was 4.23 degrees with the CSS sump running and 6.61 degrees under independent operation. The CSS line maximum swirl angle was 13.5 degrees. Average swirl angles for all tests were 2.60 degrees and 9.96 degrees for the DHR and CSS sumps, respectively. In most cases, swirl angles increased in each sump with additional screen blockages. Using the existing literature (14, 15), the swirl angles can be extrapolated to the recirculation pumps of the DHR and CSS sumps. Utilizing a conservative decay rate of 0.02 and total pipe lengths of 165 ft and 148 ft for the DHR and CSS pumps, respectively, the maximum swirl angles encountered in either line will decay to less than two degrees at the pump inlets. These swirl angles are not considered excessive and should not effect pump performance as swirl angles from combine bends can be two to three times as large (16, 17).

The inlet losses, which included screen, grate sump, and inlet entrance and reducer losses ranged from 0.58 to 0.71 ft of water for the DHR sump and from 0.48 to 0.54 ft of water for the CSS sump. Loss coefficients varied from 0.02 to 0.12 and 0.08 to 0.21 for the DHR and CSS sump, respectively, with an accuracy of ±.03. Average loss coefficients, 0.06 for the DHR sump and 0.15 for the CSS sump, were slightly different between the two sumps. Padmanabhan (19) has found that loss coefficients increase up to 80 percent in the ten degree swirl angle range and the loss coefficients are necessarily different because head losses for the two sumps are approximately the same. The loss coefficients did not change significantly with the blockage schemes or flow rates (and hence, Reynolds numbers) tested.

TABLE 4

TEST RESULTS

| Test No. | Test Parameters | Maximum Vortex | Maximum Vortex Frequency (%) | DHR SUMP Head Loss (ft of water) | DHR SUMP Loss Coefficient | DHR SUMP Swirl Angle | CSS SUMP Head Loss (ft of water) | CSS SUMP Loss Coefficient | CSS SUMP Swirl Angle |
|---|---|---|---|---|---|---|---|---|---|
| WPS-1 | F1,E1,S0,H0 | 1 | 100 | 0.60 | 0.06 | -0.84° | 0.53 | 0.18 | -8.6° |
| WPS-2 | F2,E1,S0,H0 | 1 | 100 | 0.71 | 0.05 | -2.40° | 0.48 | 0.11 | -9.0° |
| WPS-3 | F1,E1,S0,H1 | 1 | 100 | 0.58 | 0.03 | -2.96° | 0.54 | 0.21 | -8.0° |
| WPS-4 | F1,E1,S0,H2 | 2 | 46 | 0.60 | 0.07 | -0.95° | 0.50 | 0.12 | -8.6° |
| WPS-5 | F1,E1,S0,H3 | 2 | 46 | 0.60 | 0.06 | -2.59° | 0.49 | 0.08 | -9.2° |
| WPS-6 | F1,E1,S1,H3 | 2 | 15 | 0.59 | 0.04 | -3.12° | 0.50 | 0.10 | -12.3° |
| WPS-7 | F1,E1,S2,H3 | 1 | 100 | 0.62 | 0.08 | 1.96° | 0.52 | 0.15 | -1.03° |
| WPS-8 | F1,E1,S3,H3 | 2 | 51 | 0.60 | 0.06 | -4.23° | 0.52 | 0.16 | -12.0° |
| WPS-9 | F1,E1,S4,H3 | 2 | 100 | 0.62 | 0.10 | -1.53° | 0.52 | 0.15 | -11.8° |
| WPS-10 | F1,E1,S5,H3 | 2 | 100 | 0.60 | 0.06 | -0.80° | 0.52 | 0.16 | -6.0° |
| WPS-11 | F1,E1,S4*,H3 | 2 | 100 | 0.62 | 0.10 | 1.74° | 0.53 | 0.19 | -10.5° |
| WPS-12 | F1,E1,S5*,H3 | 2 | 100 | 0.63 | 0.12 | -1.27° | 0.52 | 0.17 | -11.8° |
| WPS-13 | F1,E2,S4*,H3 | 1 | 100 | 0.62 | 0.11 | 2.33° | 0.52 | 0.15 | -11.9° |
| WPS-14 | F2,E2,S4*,H3 | 1 | 100 | 0.71 | 0.05 | 2.26° | 0.48 | 0.12 | -12.2° |
| WPS-15 | F1,E2,S5*,H3 | 1 | 100 | 0.58 | 0.03 | -2.33° | 0.52 | 0.16 | -11.3° |
| WPS-16 | F2,E2,S5*,H3 | 2 | 100 | 0.70 | 0.04 | -2.78° | 0.49 | 0.14 | -13.5° |
| WPS-17 | F2,E1,S4*,H3 | 2 | 63 | 0.71 | 0.02 | 2.26° | 0.50 | 0.16 | -11.3° |
| WPS-18 | F2,E1,S5*,H3 | 2 | 49 | 0.70 | 0.03 | -2.77° | 0.49 | 0.12 | -10.2° |
| WPS-20 | F2,E1,S3,H3 | 2 | 59 | 0.70 | 0.04 | -6.31° | -- | -- | -- |
| WPS-21 | F2,E1,S4,H3 | 2 | 66 | 0.71 | 0.05 | 6.61° | -- | -- | -- |
| Average | | | | 0.64 | 0.06 | **2.60° | 0.51 | 0.15 | **9.96° |

* = Nominal 75% blocked

** = Average swirl angle is the average of the absolute values

# SUMMARY AND CONCLUSIONS

The DHR and CSS containment recirculation sumps were model tested in order to characterize their hydraulic performance. A 1:2.5 undistorted scale model was tested to ensure that adverse flow patterns did not result in improper performance of the pumps. These studies showed acceptable hydraulic performance for all combinations of flows, distributions, and screen blockages tested.

The major findings are summarized as follows:

1. Vortex activity under the worst screen blockages and flow distributions at equal velocity and Froude scale velocity was limited to surface dimples. No air drawing vortices were encountered under any test conditions. Vortices were, in general, incoherent and shifting as a result of eddies shed off the screens and trashracks.

2. Maximum swirl angle for the DHR sump was 6.61 degrees when the sump was operating independently and the CSS sump maximum swirl angle was 13.5 degrees under two sump operation and screen blockage. As the result of decay along the length of suction, pipe swirl angles encountered at both pump inlets will be less than two degrees, which is less than angles encountered by combined bends. Under these circumstances the swirl angles will not cause any adverse conditions at the pumps.

3. The average inlet loss coefficients, representing the combined effects of screens, trashrack, sump and suction pipe entrance losses, were approximately 0.15 for the DHR sump and 0.06 for the CSS sumps. No significant dependence with flow distribution and screen blockage was observed. Average head losses for all the tests were 0.64 and 0.51 ft of water for the DHR and CSS sump, respectively.

Since the literature indicates that scale effects should not be important for the scale used, these results should be transferable to the prototype. In particular, air entrainment would not be expected. Furthermore, the loss coefficients can be used to evaluate suction head availability and the swirl angle measurements can be used to predict swirl at the pump inlets. If necessary, suitable decay due to pipe length may be incorporated.

## REFERENCES

1. Murakami, M., et al., "Flow of Entrained Air in Centrifugal Pumps," 13th Congress, IAHR, Vol 2, Japan, September 1969.

2. Rouse, H., (Ed.), Engineering Hydraulics, John Wiley & Sons, 1950.

3. Dailey, J.W., and Harleman, D.R.F., Fluid Dynamics, Addison-Wesley Publishing Company, 1965.

4. Anwar, H.O., Weller, J.A., and Amphlet, M.B., "Similarity of Free-Vortex at Horizontal Intake," Journal of Hydraulic Research, IAHR 16, No. 2, 1978.

5. Daggett, L.L., and Keulegan, G.H., "Similitude Conditions in Free Surface Vortex Formations," Journal of Hydraulics Division ASCE, Vol. 100, pp. 1565-1581, November 1974.

6. Hattersley, R.T., "Hydraulic Design of Pump Intakes," Journal of the Hydraulics Division, ASCE, pp. 233-249, March 1965.

7. Reddy, Y.R., and Pickford, J., "Vortex Suppression in Stilling Pond Overflow," Journal of Hydraulics Division, ASCE, pp. 1685-1697, November 1974.

8. Harshbarger, E.D., "Bellefonte Nuclear Plant Model Tests 1:10 Scale DHR Sumps," Report No. WR28-1-88-101, Tennessee Valley Authority, September 1979.

9. Baines, W.D., and Peterson, E.G., "An Investigation of Flow Through Screens," Trans. ASME, pp. 467-477, July 1951.

10. Papworth, M., "The Effect of Screens on Flow Characteristics," British Hydromechanics Research Association, Report TN1198, November 1972.

11. Weighardt, K.E.G., "On the Resistance of Screens," The Aeronautical Quarterl , Vol. IV, February 1953.

12. Tennessee Valley Authority, "Flow Through Screens," Report No. 87-9, May 1976.

13. Padmanabhan, M.,"Hydraulic Model Studies of the Reactor Containment Building Sump, North Anna Nuclear Power Station - Unit 1," ARL Report No. 123-77/M250CF, July 1977.

14. Janik, C.R., and Padmanabhan, M., "The Effect of Swirling Flow in Pipe Friction Losses," ARL Report No. 26-81/M296KF, February 1981.

15. Baker, D.W., and Sayre, C.L., "Decay of Swirling Turbulent Flow of Compressible Fluids in Long Pipes," "Flow, Its Measurement and Control in Science and Industry," 1974.

16. Nystrom, J.B., "The Effects of Combined Bends on the Velocity Distribution and Swirl at the Inlet to a Pump," ARL Report No. 122-80/M105AF, August 1980.

17. Padmanabhan, M., "Investigation of Flow Distribution and Swirl Due to a Combined Pipe Bend," McGuire Nuclear Power Station, ARL Report No. 12-79/M208MF, December 1978.

18. Padmanabhan, M., and Hecker, G.E., "Assessment of Scale Effects on Vortexing, Swirl, and Inlet Losses in Large Sump Models," Report No. NUREG/CR-2760, SAND82-7063, May 1982.

19. Padmanabhan, M., "A Parametric Study of the Hydraulic Performance of Containment Emergency Sumps with Horizontal Double Outlets," ARL 46-82-M398F.

FIGURES

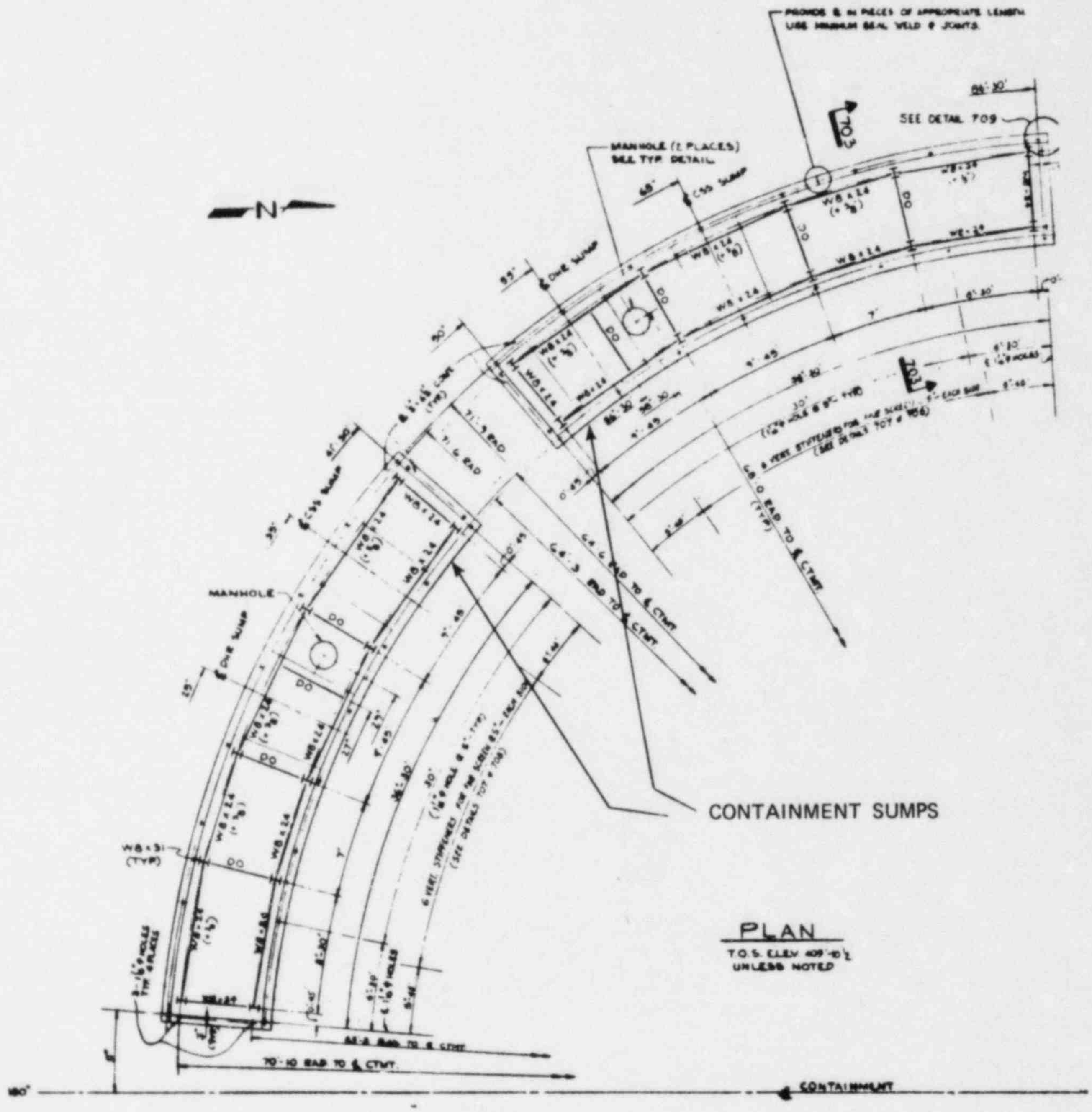


FIGURE 1 CONTAINMENT SUMP DETAILS
(From UE&C Drawing 9779-F-101378)

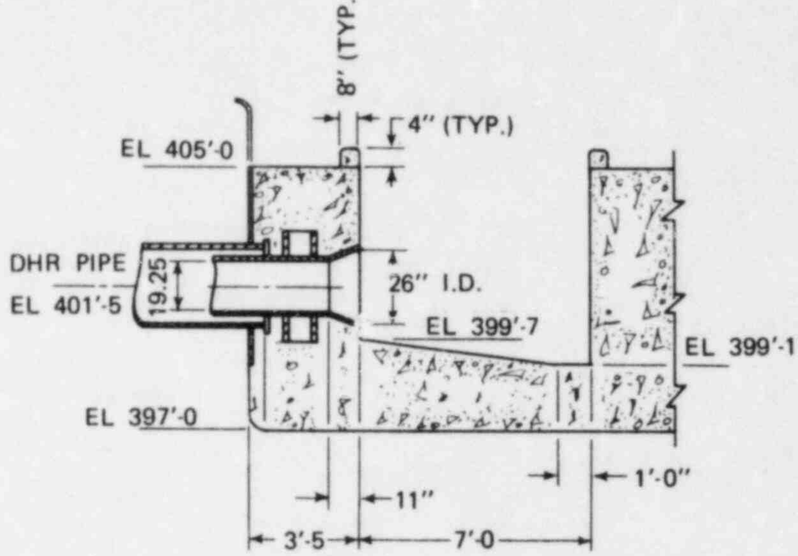


DHR SUMP PIT

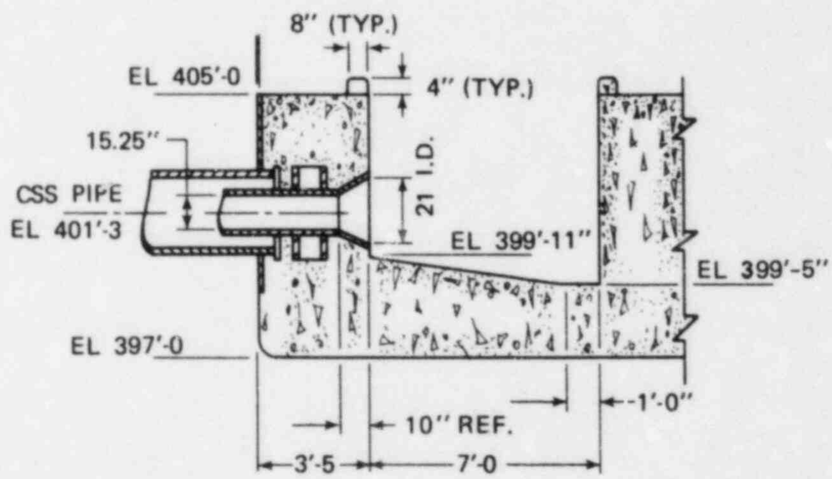


CSS SUMP PIT

FIGURE 2 SUMP DETAILS - ELEVATION VIEW

ARL

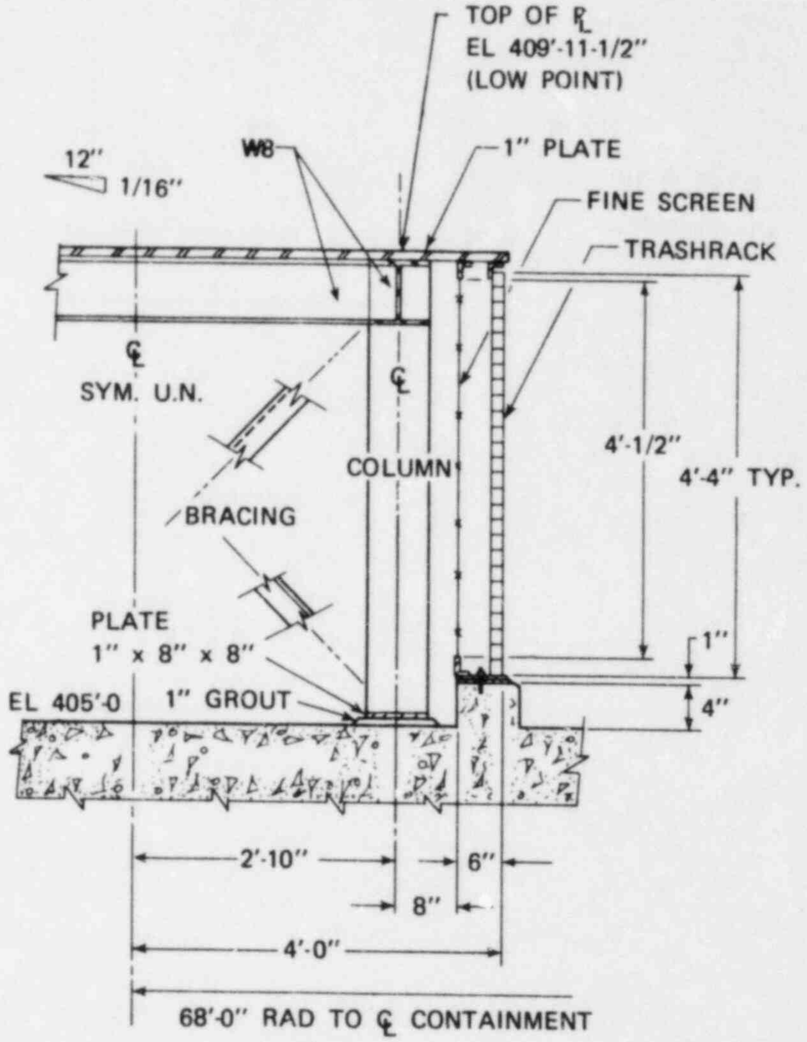


FIGURE 3 SCREEN/TRASHRACK DETAILS

ARL

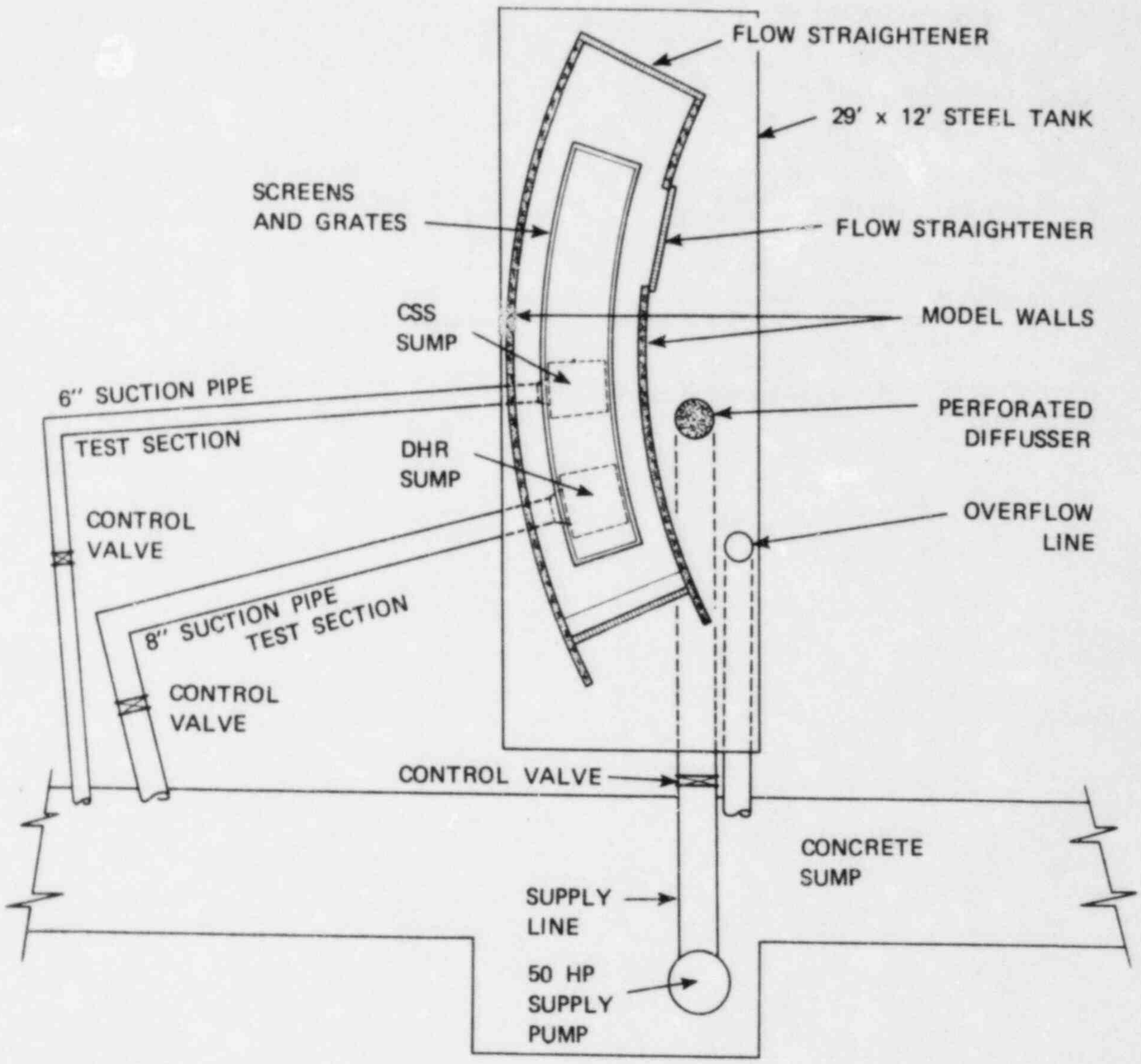


FIGURE 4 MODEL LAYOUT PLAN VIEW

ARL

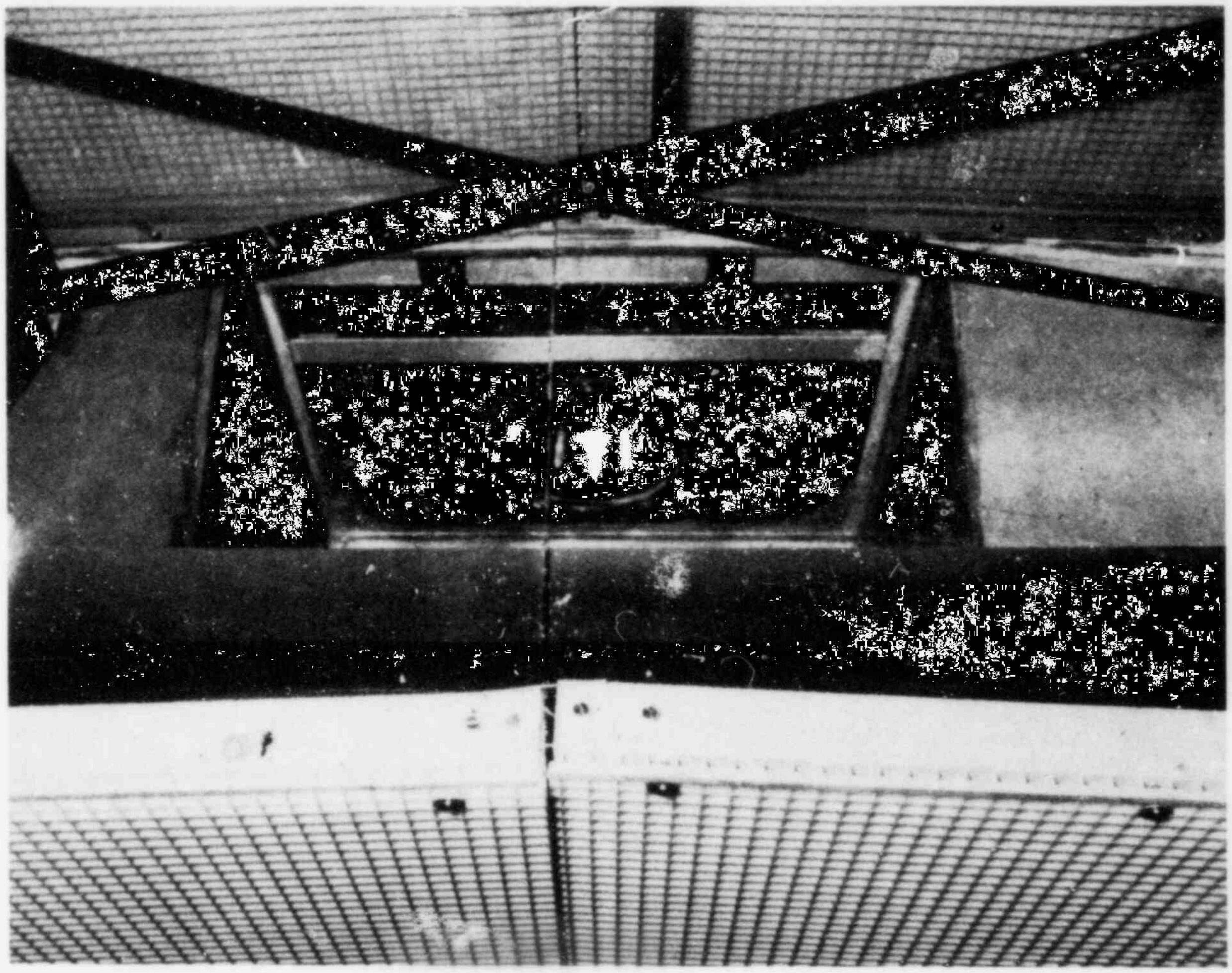

FIGURE 5 SUMP INLET AND SCREEN STRUCTURES

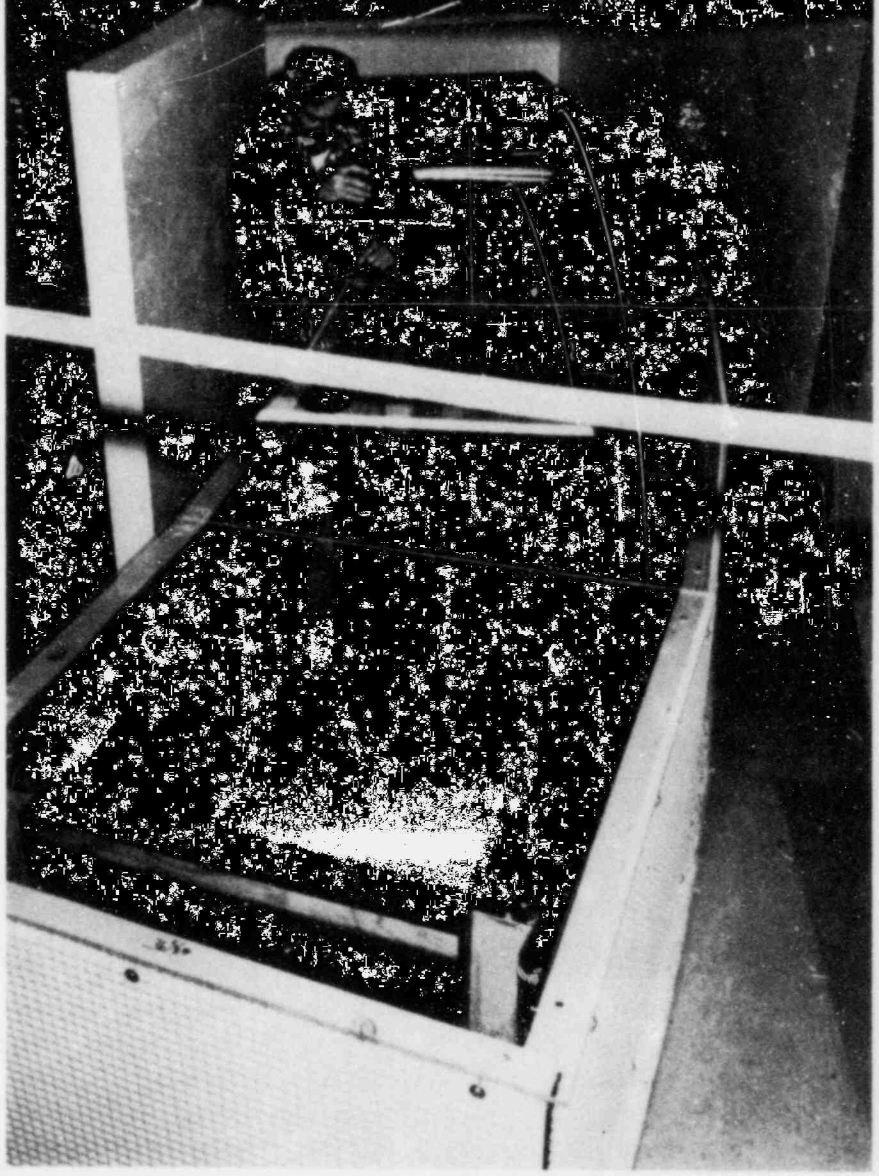

FIGURE 6   SUMP STRUCTURES - ELEVATION 405'-415'

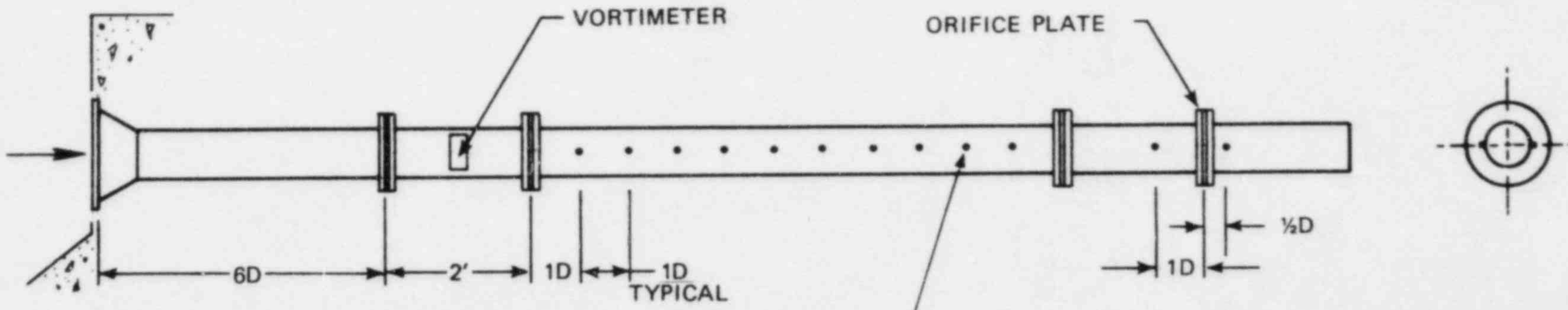


FIGURE 7 TYPICAL SUCTION PIPE TEST SECTION

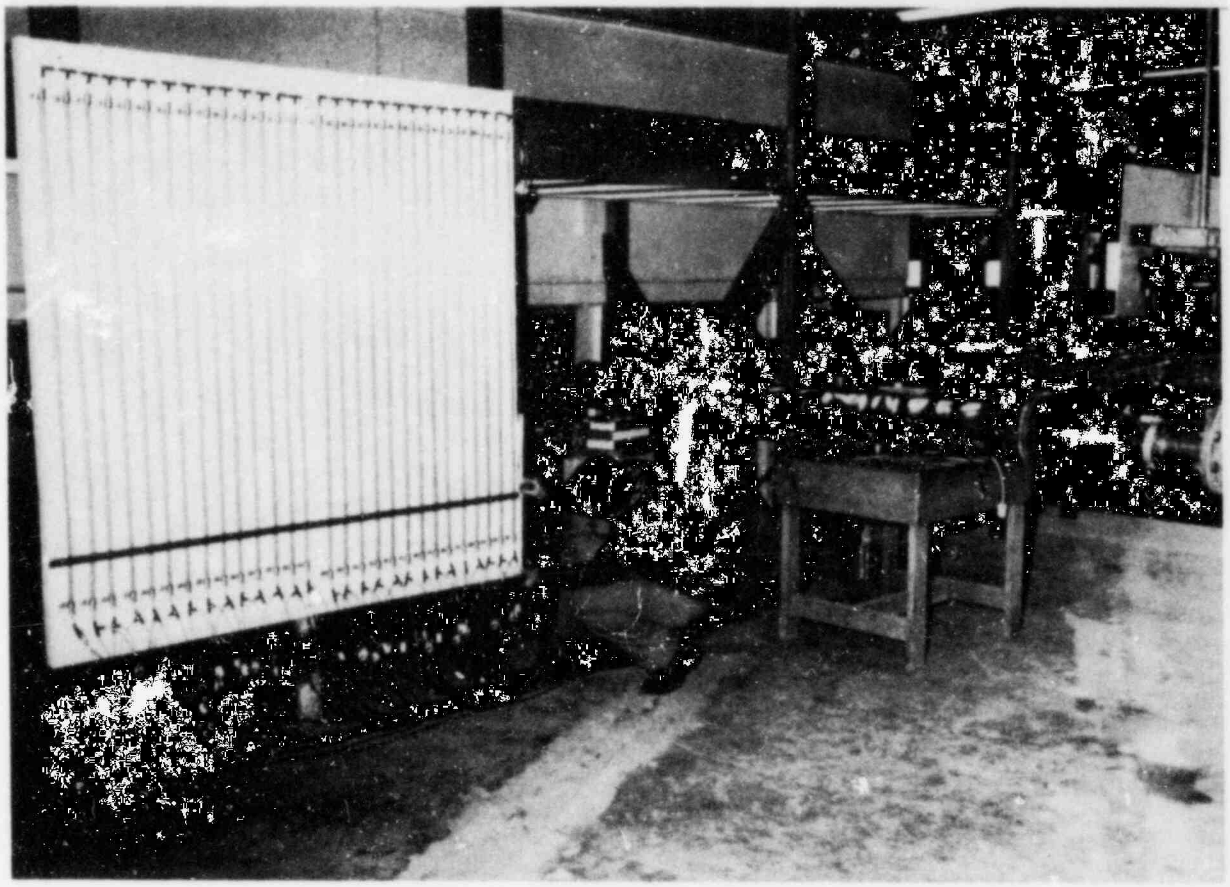

FIGURE 8 OVERALL VIEW OF TEST SECTION AND MANOMETER BOARD

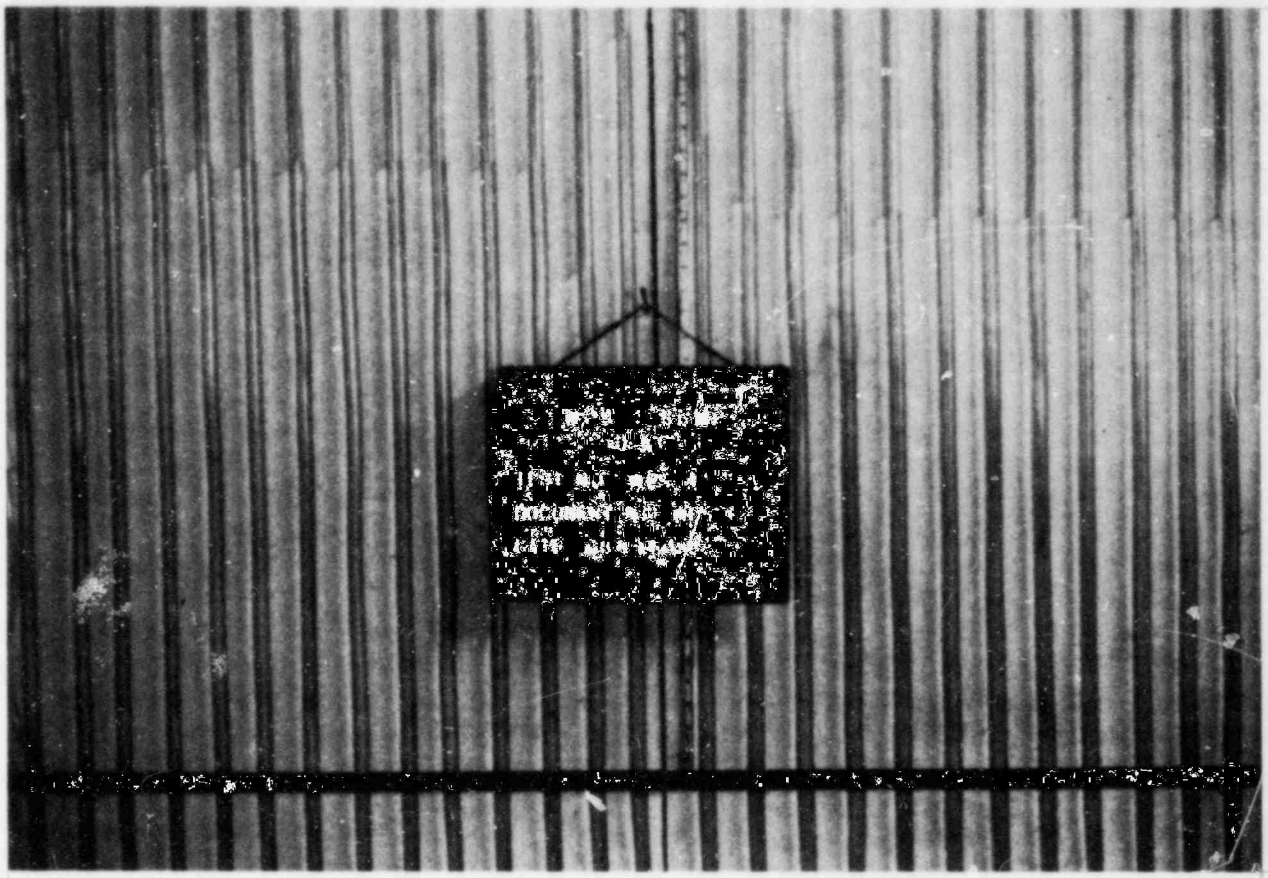

FIGURE 9 TYPICAL HYDRAULIC GRADELINE

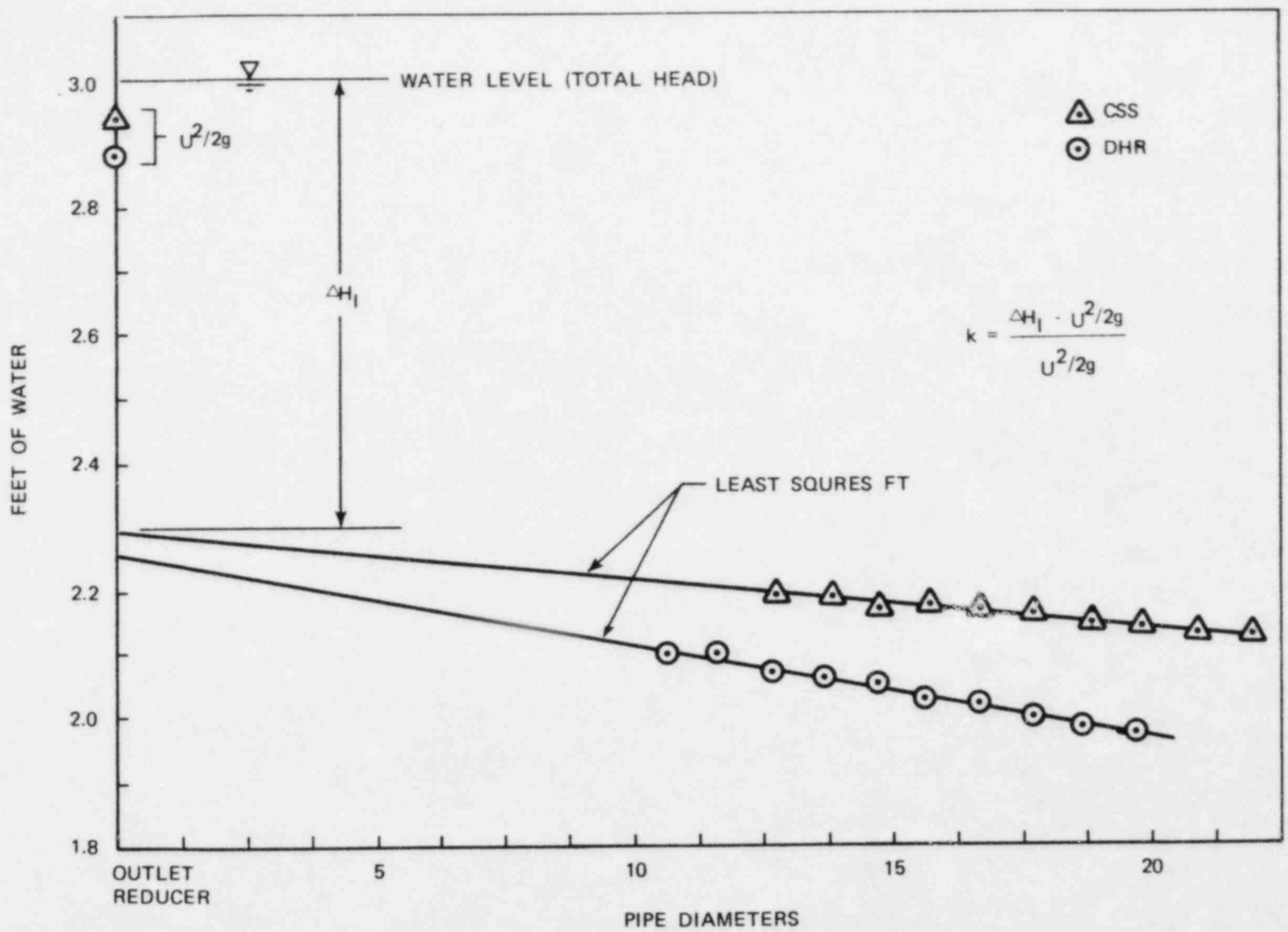


FIGURE 10 TYPICAL HYDRAULIC GRADELINE PLOT FOR DETERMINATION OF INLET LOSS

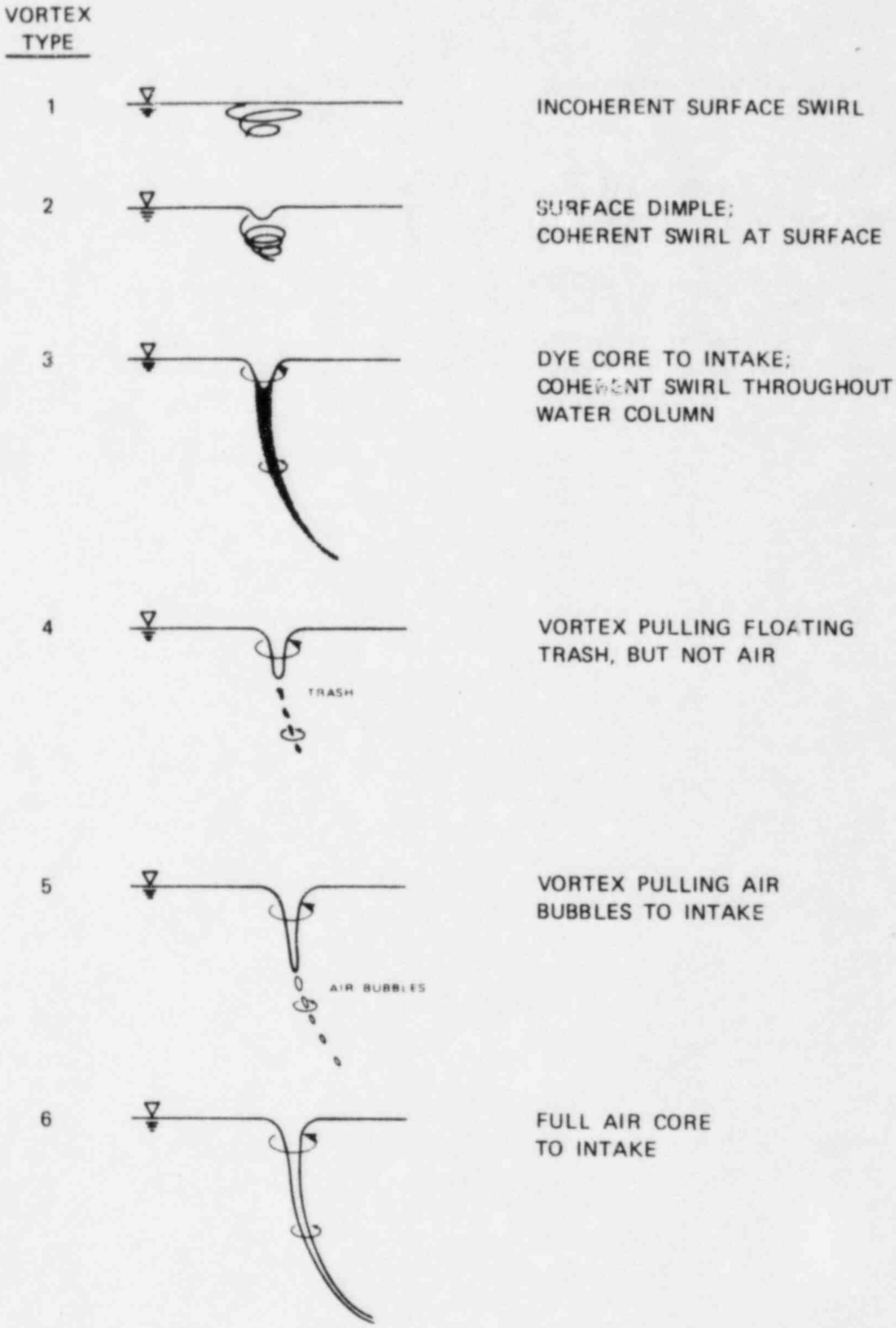


FIGURE 11 VORTEX STRENGTH CHART

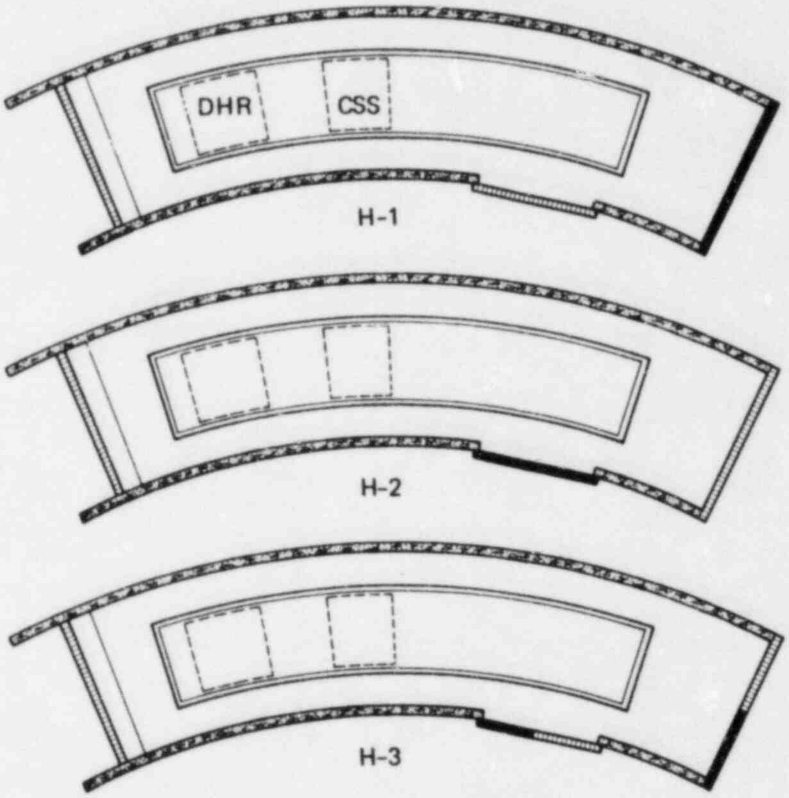


NOTE: DARK SOLID LINES INDICATE BLOCKAGE.

FIGURE 12 FLOW DISTRIBUTION SCHEMES

ARL

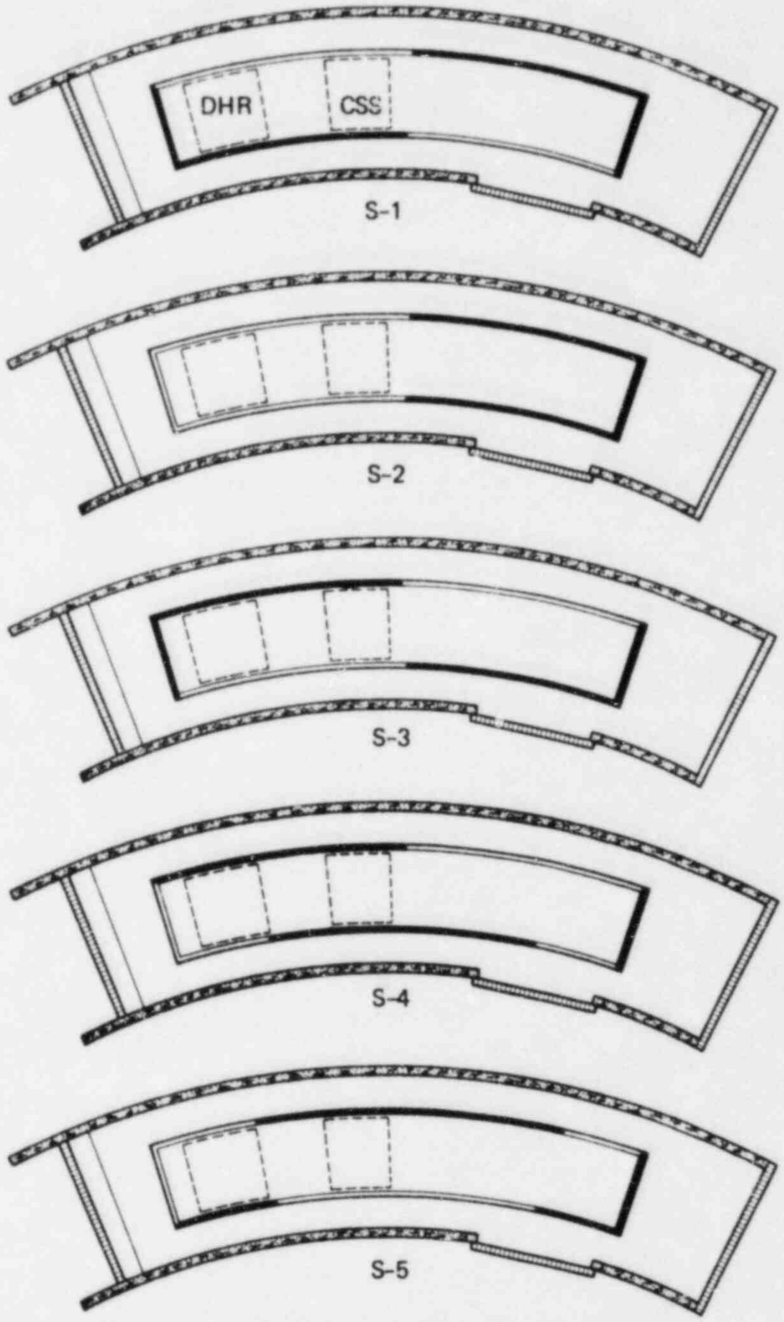


NOTE: DARK SOLID LINES INDICATE BLOCKAGE.

FIGURE 13 NOMINAL 50% SCREEN BLOCKAGE SCHEMES

ARL

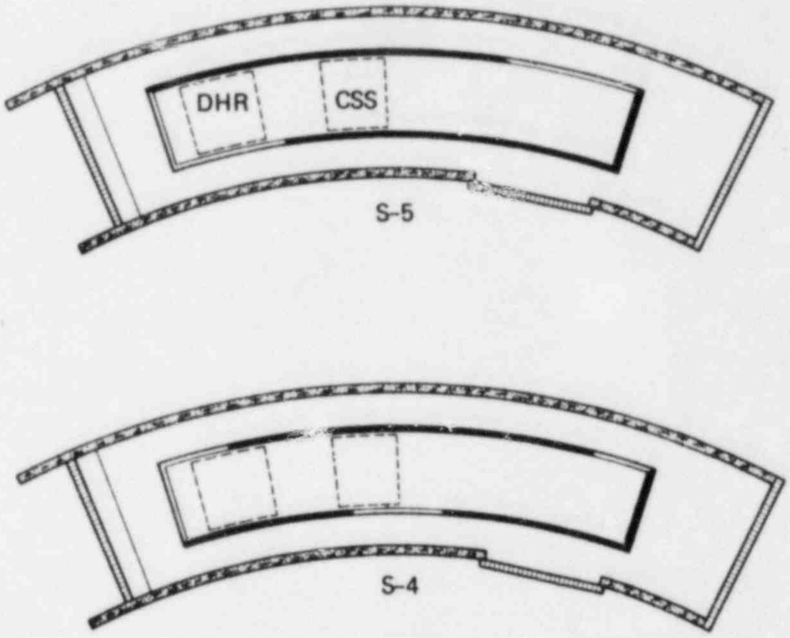


NOTE: DARK SOLID LINES INDICATE BLOCKAGE.

FIGURE 14 NOMINAL 75% SCREEN BLOCKAGE SCHEMES

ARL

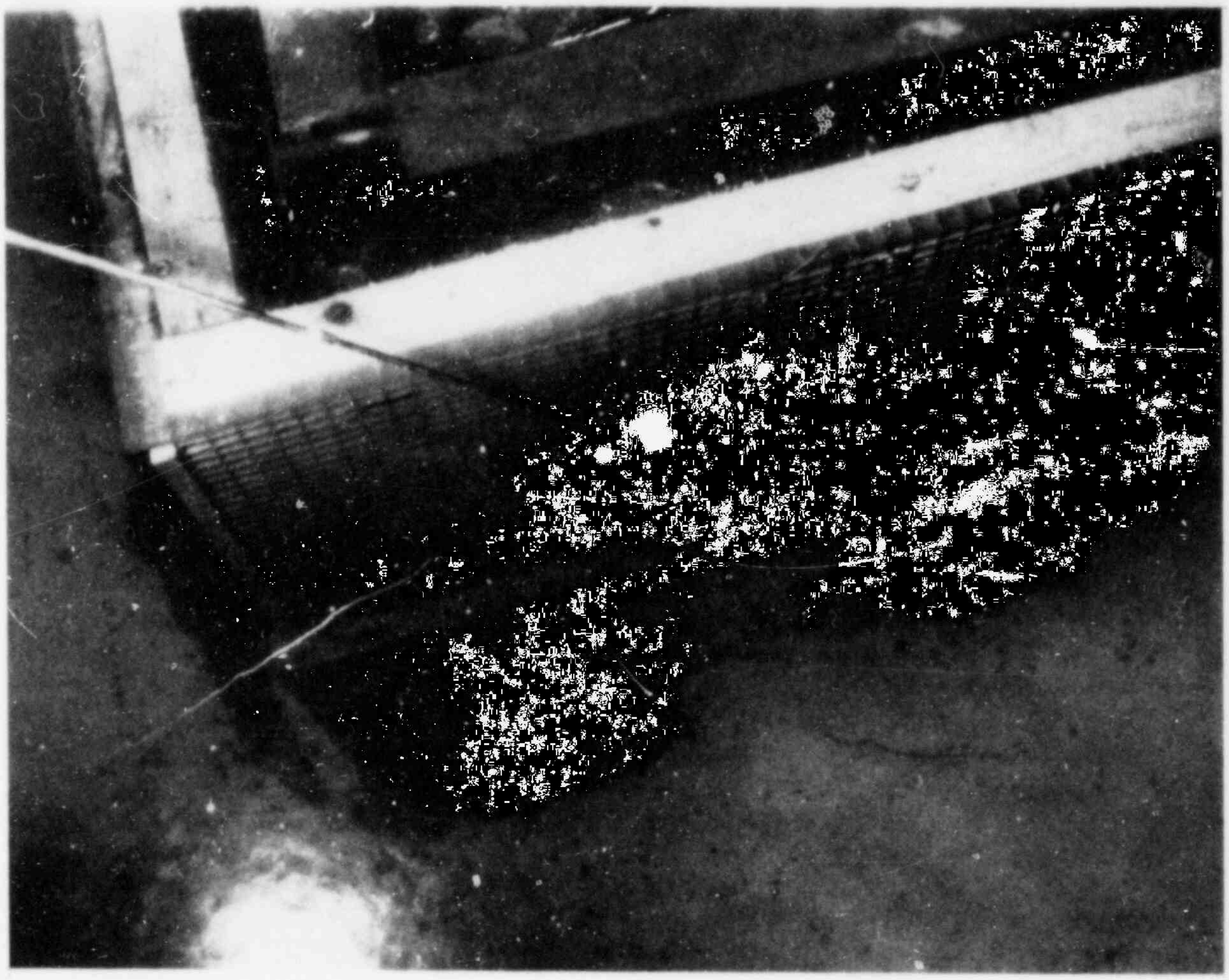

FIGURE 15 TEST 12, TYPICAL NO. 2 VORTEX

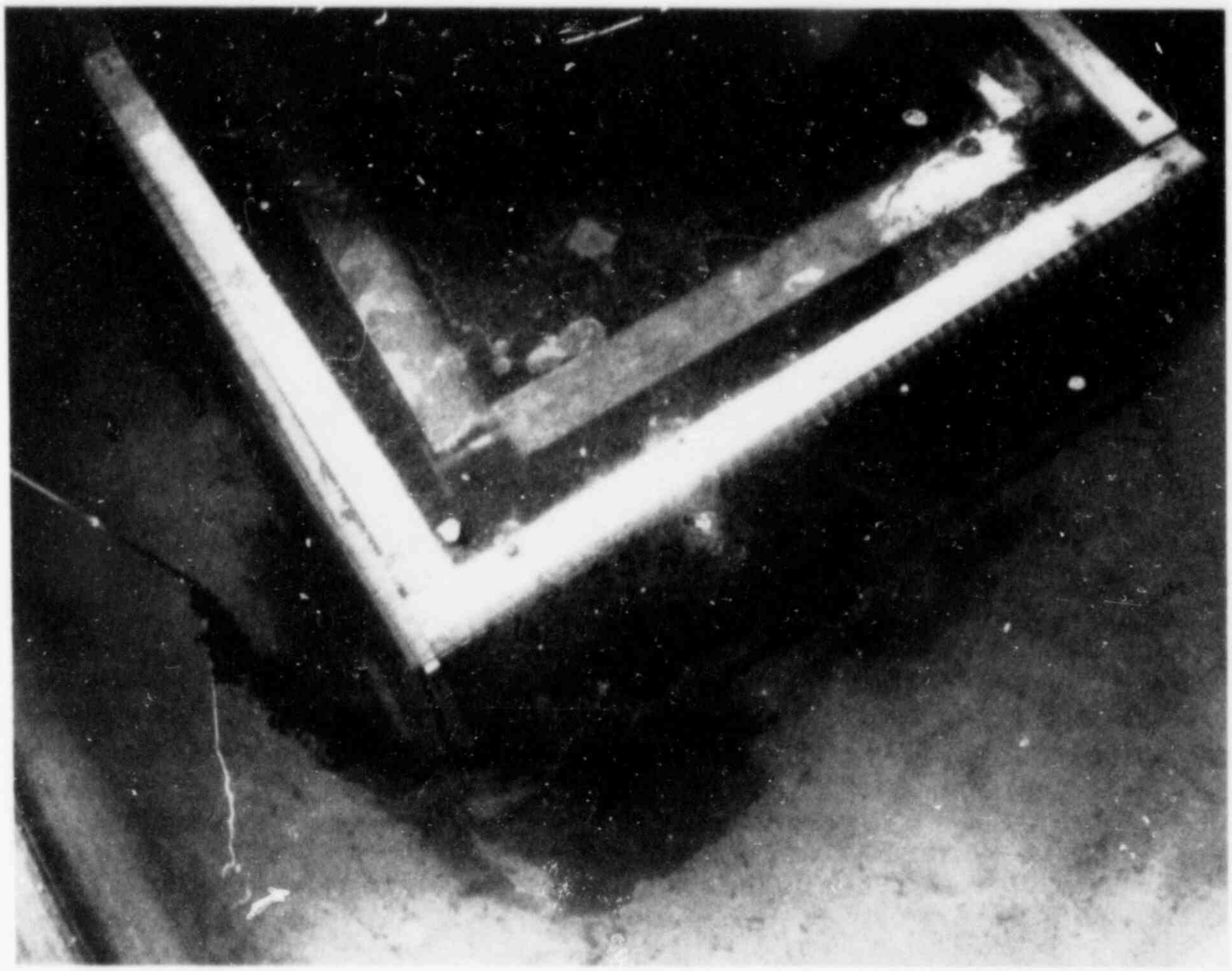

FIGURE 16 TEST 12, TYPICAL EDDY FLOW PATTERN